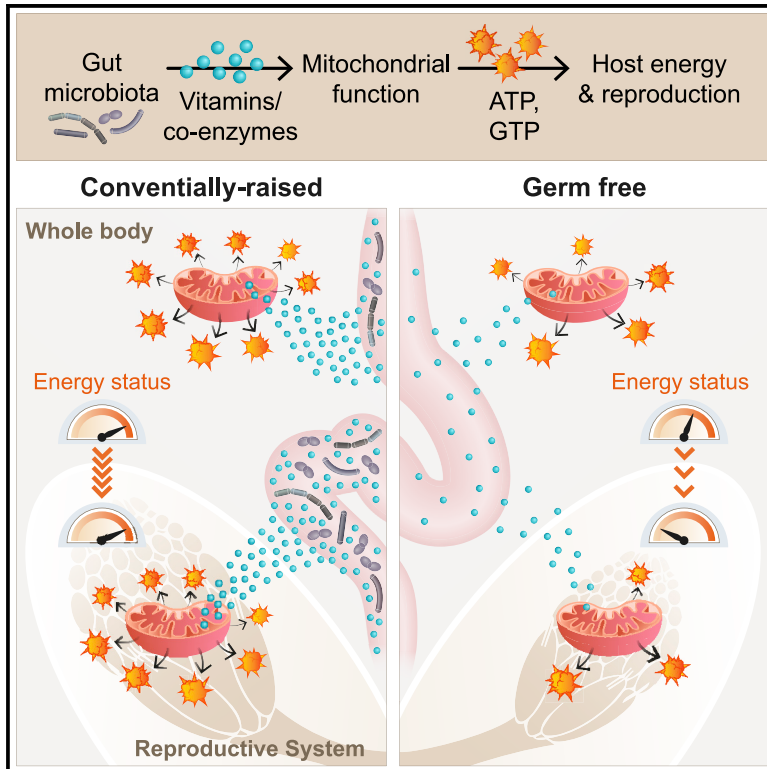


Systemic Regulation of Host Energy and Oogenesis by Microbiome-Derived Mitochondrial Coenzymes

Graphical Abstract



Authors

Yulia Gnainsky, Nofar Zfanya, Michael Elgart, ..., Sergey Malitsky, Jerzy Adamski, Yoav Soen

Correspondence

yulia.gnainsky@weizmann.ac.il

In Brief

Gnainsky et al. report a bacterial-mitochondrial axis of systemic influence, regulating host energy and reproduction by bacterial supply of vitamins required for biosynthesis of essential mitochondrial coenzymes. This was demonstrated by causal impacts of gut bacteria and bacterial-derived vitamin B2 (FAD precursor) on host mitochondrial function, ATP levels, and oogenesis.

Highlights

- Bacterial-derived mitochondrial co-enzymes regulate host energy and reproduction
- Bacterial removal decreases host FAD, mitochondrial function, and ATP levels
- Low mitochondrial function in ovarian follicle cells reduces oogenesis
- Reduced oogenesis in germ-free flies prevents drop of ATP in non-reproductive organs



Article

Systemic Regulation of Host Energy and Oogenesis by Microbiome-Derived Mitochondrial Coenzymes

Yulia Gnainsky,^{1,6,*} Nofar Zfanya,¹ Michael Elgart,² Eman Omri,¹ Alexander Brandis,³ Tevie Mehlman,³ Maxim Itkin,³ Sergey Malitsky,³ Jerzy Adamski,^{4,5} and Yoav Soen¹

¹Department of Biomolecular Sciences, Weizmann Institute of Science, 7670001 Rehovot, Israel

²Department of Medicine, Brigham and Women's Hospital, Harvard Medical Center, Boston, MA 02115, USA

³Life Sciences Core Facilities, Weizmann Institute of Science, 7670001 Rehovot, Israel

⁴Research Unit Molecular Endocrinology and Metabolism, Helmholtz Zentrum München, German Research Center for Environmental Health (GmbH), 85764 Neuherberg, Germany

⁵Department of Biochemistry, Yong Loo Lin School of Medicine, National University of Singapore, Singapore, Singapore

⁶Lead Contact

*Correspondence: yulia.gnainsky@weizmann.ac.il
<https://doi.org/10.1016/j.celrep.2020.108583>

SUMMARY

Gut microbiota have been shown to promote oogenesis and fecundity, but the mechanistic basis of remote influence on oogenesis remained unknown. Here, we report a systemic mechanism of influence mediated by bacterial-derived supply of mitochondrial coenzymes. Removal of microbiota decreased mitochondrial activity and ATP levels in the whole-body and ovary, resulting in repressed oogenesis. Similar repression was caused by RNA-based knockdown of mitochondrial function in ovarian follicle cells. Reduced mitochondrial function in germ-free (GF) females was reversed by bacterial recolonization or supplementation of riboflavin, a precursor of FAD and FMN. Metabolomics analysis of GF females revealed a decrease in oxidative phosphorylation and FAD levels and an increase in metabolites that are degraded by FAD-dependent enzymes (e.g., amino and fatty acids). Riboflavin supplementation opposed this effect, elevating mitochondrial function, ATP, and oogenesis. These findings uncover a bacterial-mitochondrial axis of influence, linking gut bacteria with systemic regulation of host energy and reproduction.

INTRODUCTION

The gut microbiota of *Drosophila melanogaster* contributes to a wide range of host functions, including regulation of growth and development (Fridmann-Sirkis et al., 2014; Reedy et al., 2019; Ridley et al., 2012; Shin et al., 2011; Storelli et al., 2011), immunity (Min and Tatar, 2018; Ryu et al., 2008; Thevenon et al., 2009), gut morphogenesis (Broderick et al., 2014; Buchon et al., 2009a, 2009b), lifespan (Brummel et al., 2004; Keebaugh et al., 2018), and behavior and mating preference (Fischer et al., 2017; Leitão-Gonçalves et al., 2017; Schretter et al., 2018; Sharon et al., 2010; Wong et al., 2017; Yuval, 2017). Some of these influences were also associated with modulation of nutrition and metabolic status of the host (Keebaugh et al., 2018; Ridley et al., 2012; Wong et al., 2014; Yamada et al., 2015). Particular examples include influence on metabolic indices (Newell and Douglas, 2014; Ridley et al., 2012; Wong et al., 2014; Yamada et al., 2015), supply of vitamins, amino acids, and short chain fatty acids (Fridmann-Sirkis et al., 2014; Neis et al., 2015; Sannino et al., 2018; Wong et al., 2014), promotion of amino acid harvesting (Yamada et al., 2015), and increased consumption of oxygen (Ridley et al., 2012). Influence on host metabolism and nutrient sensing in *Drosophila* was linked to specific gut *Acetobacter* and *Lactobacillus* species that were reported to modulate

TOR (target-of rapamycin) and insulin growth signaling (IIS) (Shin et al., 2011; Storelli et al., 2011).

Gut microbiota has also been shown to impact germline function and reproduction (Elgart and Soen, 2018; Elgart et al., 2016; Fridmann-Sirkis et al., 2014; Henriques et al., 2020; Morimoto et al., 2017; Nguyen et al., 2020). Removal of gut microbiota in *D. melanogaster* repressed oogenesis in germ-free (GF) females (Elgart et al., 2016). This effect was reversed by a sufficient increase of dietary yeast, suggesting that the repression is caused by lower levels of metabolites required for generating oocytes biomass (Drummond-Barbosa and Spradling, 2001; Hansen et al., 2013; Terashima et al., 2005). During *Drosophila* oogenesis, follicles undergo 14 morphologically distinct stages accompanied by supply of proteins, lipids, and metabolites to the developing oocyte (Sieber and Spradling, 2017; Spradling, 1993). Correlations between mitochondrial function and reproduction were also reported in human clinical studies (Chappel, 2013; May-Panloup et al., 2016), but causal influence of bacterial-derived nutrients on the host's mitochondrial function and reproduction has not been reported. Among the prime suspects for influence are B-type vitamins such as riboflavin (RbF), niacin, and thiamine, which are the precursors of mitochondrial co-enzymes (Depeint et al., 2006; Fridmann-Sirkis et al., 2014; LeBlanc et al., 2013; Wong et al., 2014). Two essential co-enzymes, flavin adenine dinucleotide (FAD) and flavin mononucleotide (FMN), are derived



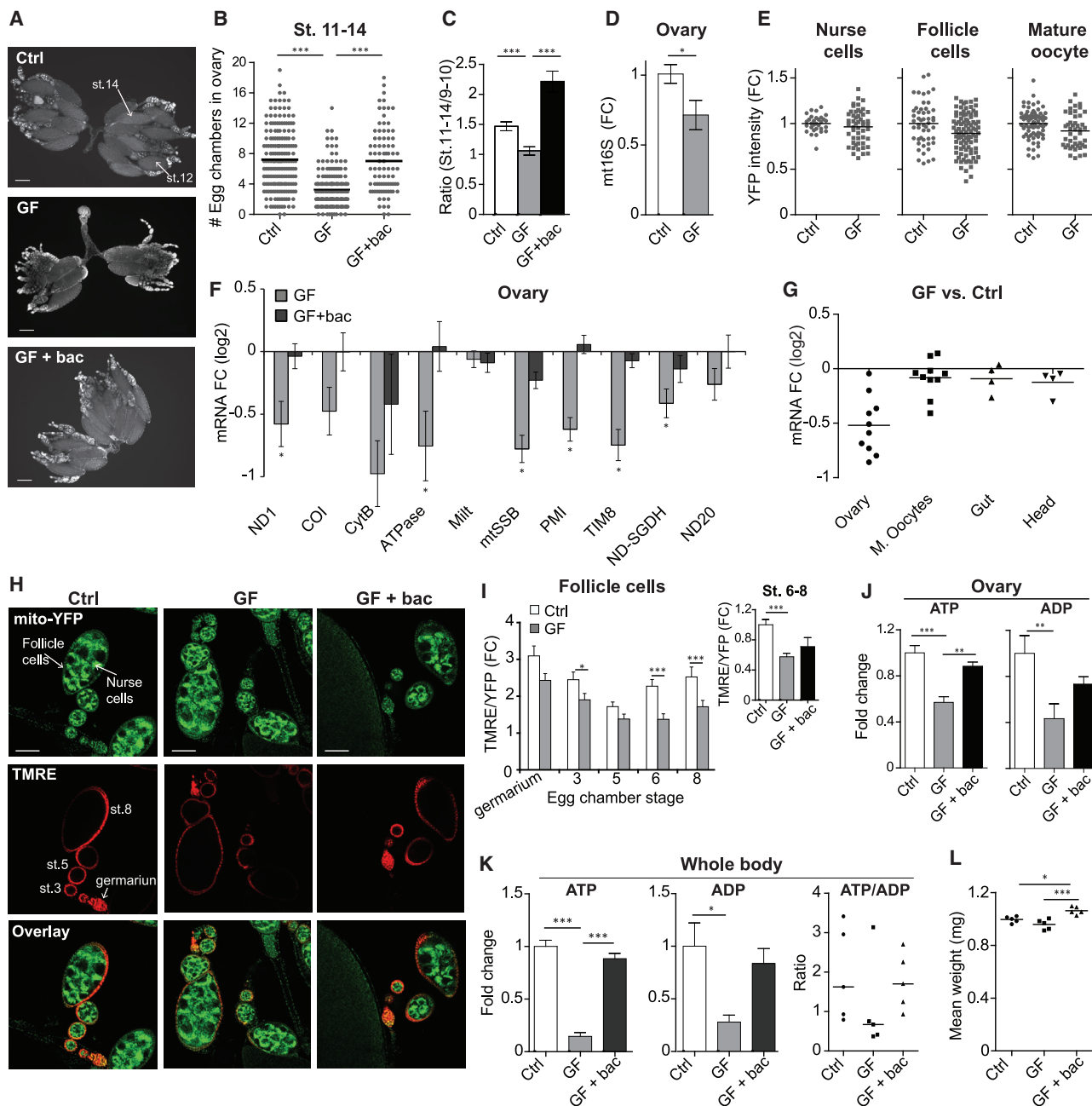


Figure 1. Reduced Mitochondrial Function in Ovaries (Ovs) of Germ-Free (GF) Females versus Control

(A) Representative images of DAPI-stained ovaries in the following cases of 6-day yw females: conventionally raised (Ctrl), GF, and mono-association with bacteria from a single colony (*Col1*) of an *Acetobacter* isolate (GF + bac). Scale bar, 200 μ m.

(B and C) Numbers of stages 11–14 egg chambers in ovary (B) and the ratio between the numbers in stages 11–14 and 9–10 (C). Data are presented as medians (B) and mean \pm SEM (C) of 5 independent experiments, each with $n > 20$ ovaries; *** $p < 0.001$ (Kruskal-Wallis with Dunn's multiple comparisons test).

(D) Fold change (FC) of mitochondrial DNA content in whole ovaries, determined by qPCR analysis of DNA coding for mitochondrial 16S (*mt16S*) normalized by *actin* DNA. Mean \pm SEM; $n = 7-8$, with 10 ovaries per sample; * $p < 0.05$ (t test).

(E) FC of YFP fluorescence intensity in follicle and nurse cells of stages 6–8 egg chambers and in mature oocytes of Ctrl and GF mito-EYFP females. Mean; $n > 30$.

(F) mRNA FC (log2) of mitochondria-encoded (*ND1*, *COI*, *CytB*, and *ATPase*) and nucleus-encoded mitochondrial genes (*Milt*, *mtSSB*, *Tim8*, *PMI*, *ND-SGDH*, and *ND-20*) in whole ovaries versus Ctrl for the cases in (A). Mean \pm SEM of 3 independent experiments; $n = 9$ each with 10 ovaries; * $p < 0.05$ (t test). *COI*, cytochrome C oxidase; *ND1*, NADH-ubiquinone oxidoreductase chain 1; *cytB*, cytochrome B; *Milt*, Milton; *mtSSB*, mitochondrial single stranded DNA-binding protein; *PMI*, protein of the mitochondrial inner membrane; *ND-SGDH*, NADH dehydrogenase (ubiquinone) SGD subunit; *ND-20*, NADH dehydrogenase (ubiquinone) 20 kDa subunit.

(legend continued on next page)

from RbF-vitamin B2 (Bafunno et al., 2004; Udhayabanu et al., 2017). RbF cannot be synthesized by the host and can only be supplied by symbiotic gut bacteria or via the diet. This suggests that the growth retardation and oogenesis repression in GF females (Elgart et al., 2016; Fridmann-Sirkis et al., 2014) are caused by insufficient levels of RbF and/or other bacterial-derived vitamins. The hypothesized influence of bacterial vitamins on the host's mitochondria can provide a unifying mechanistic explanation for previously reported involvement of gut bacteria in insulin signaling (Shin et al., 2011) and nutrient sensing (Storelli et al., 2011). Here, we provide direct evidence in support of this hypothesis. We show that removal of gut bacteria reduces RbF (and FAD) levels and decreases the levels of metabolites in the citric acid cycle, glycolysis, and electron transport chain pathways. These changes are accompanied by global reduction in ATP (and GTP) and lower mitochondrial activity in the follicle cells of developing oocytes. We further show that follicle-cell-specific reduction of mitochondrial gene dosage is sufficient to represses oogenesis in conventionally raised females, and the negative impact of bacterial removal on host mitochondrial function and oogenesis are alleviated by supplementation of RbF. These results demonstrate a bacterial-mitochondrial axis regulating host energy and oogenesis via bacterial supply of metabolic precursors of mitochondrial coenzymes.

RESULTS

Removal of Gut Microbiota Downregulates Mitochondrial Genes in the Ovary

To investigate how gut-residing bacteria influence oocyte development in the ovary, we removed the gut microbiota by egg dechoriation and placed these GF eggs on standard diet under sterile conditions. As demonstrated by Elgart et al. (2016), the number of late-stage oocytes in ovaries of GF females was lower compared to conventionally raised (control) females (Figures 1A–1C) and was fully restored by supplementation of an *Acetobacter* spp., *Col1* isolated from our stocks (Fridmann-Sirkis et al., 2014). To investigate if the reduced oogenesis in GF females is mediated by changes in the host's mitochondria, we first analyzed mitochondrial content by measuring 16S mitochondrial DNA. Analysis of whole ovaries at day 6 post-eclosion revealed lower levels of mitochondrial DNA in GF versus control females (Figure 1D). A smaller decrease of oogenesis and mitochondrial DNA content was already noticed at day 2, prior to maturation of the ovary (Figures S1A–S1C). Compartment-specific analysis of mitochondrial content in nurse cells, follicle cells, and mature

oocytes of mito-EYFP females, revealed only mild differences between GF and control (Figure 1E), suggesting that the lower level of mitochondrial DNA in ovaries of GF is mainly due to the reduced number of late-stage oocytes.

To test if the removal of gut bacteria influences the expression of mitochondrial genes, we selected a representative panel of mitochondrial transcripts (both mitochondrially encoded and nuclear-encoded) and analyzed their levels in GF versus control. Most of the mitochondrial genes were downregulated in whole ovaries of GF females at days 2 and 6 (Figures 1F and S1D), but not in mature oocytes of GF females versus controls (Figure 1G). Analysis of gut and head tissues revealed only mild reduction (Figure 1G), suggesting that the impact of bacterial removal on the expression of mitochondrial genes is most pronounced in developing egg chambers. Much like the reversibility of repressed oogenesis (Figures 1B and 1C), the downregulation of mitochondrial genes in the ovary was fully reversed by supplementing bacteria from an *Acetobacter* isolate, *Col1* (Figure 1E).

Reduced Mitochondrial Function and ATP Production in GF Females

To determine if the removal of gut bacteria also influences the activity of the mitochondria in the host, we stained ovaries of mito-EYFP flies with the TMRE indicator of mitochondrial membrane potential (Parker et al., 2017). We used the TMRE/YFP ratio as an intrinsic measure of mitochondrial function that is independent of mitochondrial content. Stage-specific analysis of dissected ovaries revealed lower levels of TMRE/YFP in somatic follicle cells surrounding the egg chambers of GF females versus controls (Figures 1H and 1I). This reduction in mitochondrial membrane potential was observed in various states, from the germarium up to stage 8 egg chambers, but was most prominent at stages 6–8. As independent assessment of mitochondrial output, we measured the ATP and ADP levels using quantitative liquid chromatography mass spectrometry (qLC-MS). The levels of both ATP and ADP were significantly lower in whole ovaries of day-6 GF females versus controls (Figure 1J). Substantially lower levels of ATP and ADP (as well as GTP and GDP) were also observed in whole body samples of GF females (Figures 1K and S2A), including after normalization by total mass (Figure S2B). A smaller reduction in ATP was observed in mature oocytes and dissected heads of GF females (Figure S2C). These changes were consistent with mild decrease in overall weight of GF females versus controls (Figure 1L), suggesting a systemic impact of bacterial removal on ATP production in the host. Additional support was obtained significantly lower levels of ATP and

(G) mRNA FC (log2) of mitochondrial genes in: ovary, $n = 9$, each with 10 ovaries; mature oocytes (M. Oocytes), $n = 13$, each with ~50 oocytes; gut, $n = 12$, each with 10 guts; and head, $n = 8$, with 10 heads each.

(H) Representative images of TMRE-stained ovarioles of day-6 mito-EYFP females. green, YFP-labeled mitochondria; red, TMRE. Scale bar, 50 μ m.

(I) Ratio between TMRE and YFP intensity in follicle cells of various stages of egg chambers (up to stage 8). Inset: average TMRE/EYFP FC in stages 6–8. Mean \pm SEM; $n = 20$ –80, based on 3 independent experiments; * $p < 0.05$, *** $p < 0.001$ (Kruskal Wallis with Dunn's multiple comparisons test).

(J) FC of ATP and ADP measured by qLC-MS in isolated ovaries for the cases in (A). Mean \pm SEM; $n = 9$ with 10 ovaries per sample, based on 3 independent experiments; *** $p < 0.001$, ** $p < 0.01$ (ANOVA with Tukey's multiple comparisons test).

(K) Fold-change of whole-body levels of ATP and ADP versus Ctrl (left and right) and the distribution of ATP/ADP ratios. Mean \pm SEM; $n = 5$ with 50 flies per sample; * $p < 0.05$, *** $p < 0.001$ (ANOVA with Tukey's multiple comparisons test).

(L) Mean female weight (mg) for the cases in (A). * $p < 0.05$, *** $p < 0.001$ (ANOVA with Tukey's multiple comparisons test).

See also Figure S1.

ADP in GF males versus controls (Figure S2D) as well as by small reduction in weight of GF males (Figure S2E). Altogether, these findings provide evidence for two main impacts of bacterial removal: systemic decrease in ATP production by reproductive and non-reproductive organs of the host, and substantial attenuation of mitochondrial activity in follicle cells of the developing egg chamber.

Reduced Mitochondrial Function in Somatic Follicle Cells Suffices to Repress Oogenesis

To investigate if the reduction in mitochondrial activity can account for the repressed oogenesis in GF females, we inhibited mitochondrial function in flies with intact gut microbiota and analyzed the influence on oogenesis. We first examined the impact of exposure to rotenone, a chemical inhibitor of the mitochondrial complex I. To avoid significant disruption of gut microbiota, we identified concentrations of rotenone that are still permissive for bacterial growth (Figure 2A). 3 days of female exposure to 25 μ M of rotenone had almost no effect on the bacteria, but was sufficient to repress oogenesis, as indicated by the substantial reduction in the number of oocytes at stages 11–14 (Figures 2B and S3A). Removal of rotenone by transfer to rotenone-free diet for 3 days led to complete recovery of oogenesis (similar to the rescue of oogenesis by supplementing gut bacteria to the diet of GF females). Analysis in whole ovaries of rotenone-treated versus control females revealed a signature of changes in mitochondrial transcripts that were highly correlated with the gene-specific changes in GF females versus controls (Figures 2C and 2D). Rotenone treatment also mimicked the (stage-specific) impact of bacterial removal on the mitochondrial function in follicle cells (Figures 2E–2G) as well as on the levels of ATP and ADP (Figure 2F versus Figure 1J).

Because rotenone was provided systemically (via the diet), the repression of oogenesis in rotenone-exposed females could be mediated by direct and/or indirect mechanisms. We therefore sought to determine if tissue-specific loss of mitochondrial function in somatic follicle cells is enough to repress oogenesis. We used *traffic jam-GAL4 (Tj)* to express RNAi against *ND-20* and *SGDH* subunits of mitochondrial complex I, specifically in somatic follicle cells (Tj). qPCR analysis of the *ND-20* and *SGDH* levels in the *Tj>siND-20* and *Tj>siSGDH* versus *Tj>siCtrl* RNAi line revealed 40%–50% knockdown efficiency (Figure 2I). The follicle-specific knockdown of either genes was sufficient to repress the mitochondrial membrane potential (Figures 2J and 2K) and to substantially reduce the number and fraction of egg chambers in stages 11–14 versus stages 9–10 (Figure 2L). In contrast, germline-specific RNAi (using *NOS>siND-20* and *NOS>siSGDH*) achieved comparable levels of knockdown (Figure S3B versus Figure 2I) but had no more than a negligible impact on oogenesis (Figure S3C).

RbF Increases Oogenesis and Mitochondrial Function in GF Females

The resemblance between the outcome of nutritional deficiency (Terashima et al., 2005) and the repression of oogenesis in GF females that is reversed by sufficient addition of dietary yeast (Elgart et al., 2016) suggested that bacterial removal result in nutritional deficiency that represses the oogenesis. The lower

mitochondrial function and ATP levels in GF flies led us to suspect a deficiency in mitochondrial coenzymes that are not synthesized by the host but can be derived from bacterial metabolites. A particularly promising candidate is vitamin B2 (RbF), a precursor for two essential mitochondrial co-enzymes, FAD and FMN (Depeint et al., 2006). We therefore investigated the effect of dietary RbF on mitochondrial function and oogenesis in GF females. Supplementation of RbF to the diet increased the number and fraction of egg chambers in stages 11–14 of GF females (Figures 3A–3C). Tissue-specific analysis of TMRE/EYFP further revealed complete restoration of the mitochondrial membrane potential in follicle cells of the developing egg chambers of GF females (Figures 3D and 3E). This was accompanied by partial, but nonetheless significant, rescue of ATP levels in the ovary and whole body of GF females (Figures 3F and 3G). Altogether, these findings revealed systemic regulation of oogenesis by bacterial supply of a co-enzyme precursors that are required for mitochondrial function.

Metabolomics Analysis Supports Global Reduction of Oxidative Phosphorylation in GF Females

Next, we sought to investigate how the metabolic state of the host is affected by the impact of bacterial removal on the host mitochondrial function and ATP production. To analyze bacterial influences on a wide range of metabolites, we used targeted LC-MS to profile 197 polar metabolites and 151 lipids in dissected ovaries and whole-body GF versus control females on day 6.

Global clustering of fold-changes and principal-component analysis (PCA) revealed metabolome-wide shifts that were reversed by supplementing native gut bacteria to the diet of GF females (Figures S4 and S5). More focused analysis of bacterially supplied vitamins and respective mitochondrial coenzymes revealed significantly lower levels of RbF and FAD in whole-body and ovaries of GF females versus controls (Figure 4A and 4B). The levels of 4-pyridoxic acid (a vitamin B6 derivative) and biotin (B7) were also lower in whole body samples of GF females and ovaries of GF females were deficient in all the B-type vitamins that were detected, including thiamine pyrophosphate (a B1 derivative), nicotinate (B3), and pantothenate (B5) (Figure S6A). Because FAD is required for enzymatic breakdown (or chemical modification) of a wide range of metabolites, we evaluated the effects of bacterial removal on the distinct subsets of FAD-dependent and FAD-independent metabolites. Although almost all the FAD-dependent metabolites were higher in whole body of GF females versus controls, FAD-independent metabolites had no preferred direction of change (Figure 4C). Pathway enrichment analysis of differential metabolites in GF females versus control further revealed a significant decrease of metabolites belonging to the main pathways of energy production (Figures 4D and S6B), including the citric acid cycle (TCA), glycolysis, pentose phosphate, and electron transport chain. These changes were also consistent with lower whole-body level of nucleotides involved in energy transfer, such as ATP, GTP, CTP, and UTP, but not in the respective nucleosides, adenosine, guanosine, cytidine, and uridine (Figures S2B and S6C). The significant trend toward lower levels of TCA, glycolysis, and pentose phosphate metabolites was noted in both whole body and ovaries of GF females, with an exception of whole body levels

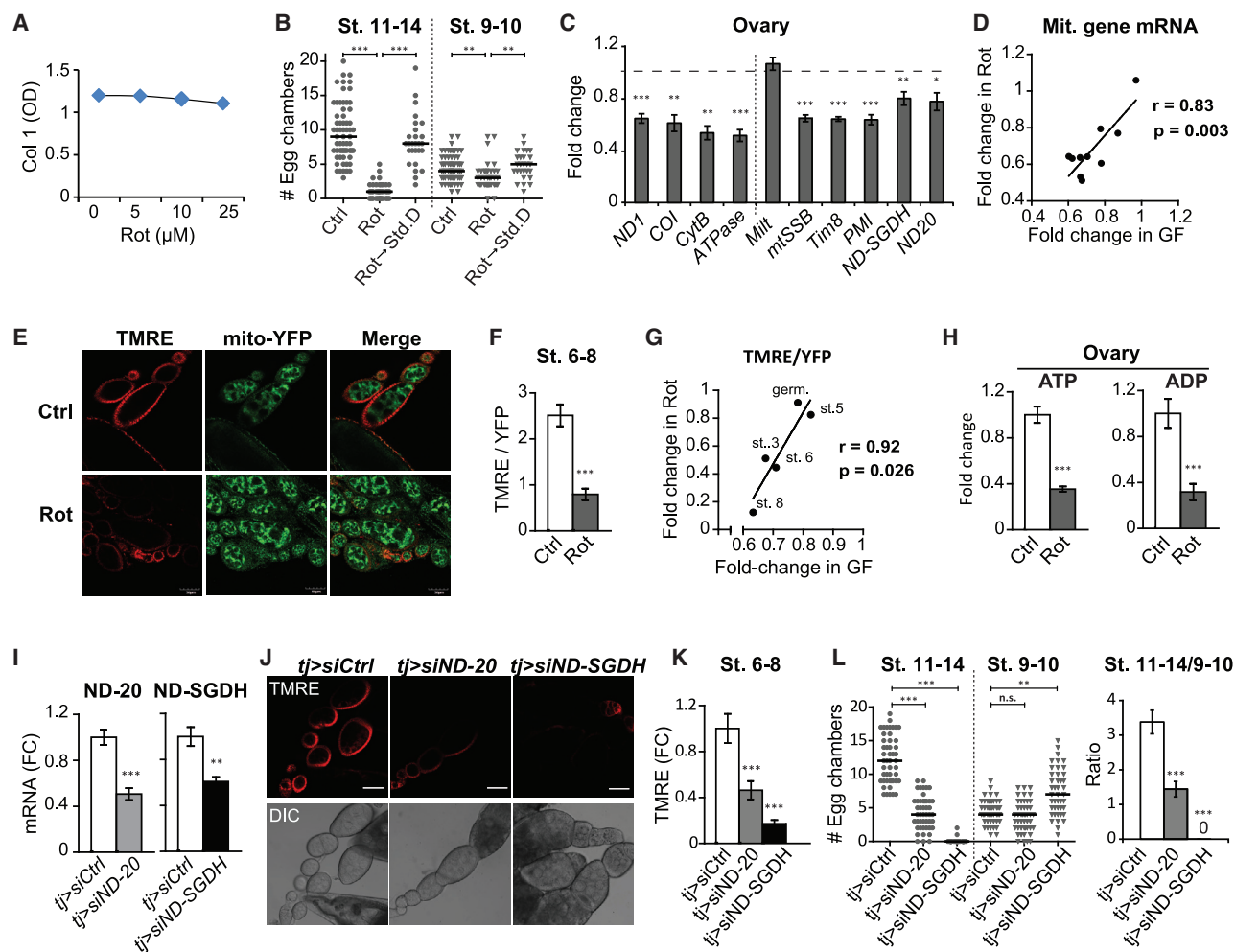


Figure 2. Repressed Oogenesis by Either Global or Follicle-Cell-Specific Inhibition of Mitochondria

(A) Bacterial density (OD) of *Col1* (gut *Acetobacter* isolate) exposed to the indicated concentration of rotenone.

(B) Number of egg chambers at stages 11–14 and 9–10, analyzed in conventionally raised females (yw) for the following cases: no treatment (Ctrl), rotenone exposure (25 μ M) from days 3–6, with and without subsequent transfer to rotenone-free diet for 3 additional days (Rot and Rot \rightarrow Std. Diet, respectively). $n > 28$ ovaries; ** $p < 0.01$, *** $p < 0.001$ (ANOVA with Tukey's multiple comparison test).

(C) mRNA FC of mitochondrial genes versus Ctrl, based on qPCR analysis of ovaries of 6-day untreated (Ctrl) and rotenone-exposed (Rot) OrR females. Mitochondria-encoded (left) and nucleus-encoded genes (right). Mean \pm SEM, $n \geq 5$ (7 ovaries per sample); * $p < 0.05$, ** $p < 0.01$, *** $p < 0.001$ (t test).

(D) mRNA FC of mitochondrial genes in the ovary following rotenone treatment versus no treatment (y axis) plotted against the respective FC in GF versus conventionally raised females (x axis). Each dot corresponds to a particular gene. p refers to the significance of the Pearson correlation coefficient (r).

(E and F) Representative images of TMRE-stained ovarioles (E) and the respective TMRE/EYFP ratios follicle cells of stages 6–8 egg chambers (F) of 6-day rotenone-treated (Rot) and untreated mito-EYFP females (Ctrl). green, EYFP-labeled mitochondria; red, TMRE; Mean \pm SEM; ~ 32 egg chambers per case; *** $p < 0.001$ (Mann-Whitney test). Scale bar, 50 μ m.

(G) Same as (D) for average TMRE/EYFP FC in follicle cells at the indicated stages.

(H) ATP and ADP FC in ovaries of untreated (Ctrl) and rotenone-treated (Rot) OrR females. Mean \pm SE; $n = 6$ with 10 ovaries/sample; *** $p < 0.001$ (t test).

(I) mRNA FC of *ND-20* and *ND-SGDH* in dissected ovaries of *tj>siND-20* and *tj>siND-SGDH* versus *tj>siCtrl* females. Egg chambers over stage 9 were removed prior to analysis. Means \pm SE; $n \geq 5$ (7 ovaries per sample); ** $p < 0.01$, *** $p < 0.001$ (t test).

(J) Representative images of TMRE-stained ovarioles (red) of 6-day *tj>siCtrl*, *tj>siND-20* and *tj>siND-SGDH* females. Scale bar, 50 μ m.

(K) TMRE FC in follicle cells in stages 6–8 egg chambers, corresponding to the cases in (J). Mean \pm SEM; $n = 15$ –30 egg chambers. *** $p < 0.001$ versus *tj>siCtrl* (ANOVA with Tukey's multiple comparisons test).

(L) Number of egg chambers at stages 11–14 and 9–10 (left) and their ratios (right) in ovaries of *tj>siCtrl*, *tj>siND-20*, and *tj>siND-SGDH* females. $n = 42$ –48 ovaries; *** $p < 0.001$ versus *tj>siCtrl* (ANOVA with Tukey's multiple comparisons test).

See also Figures S2 and S3.

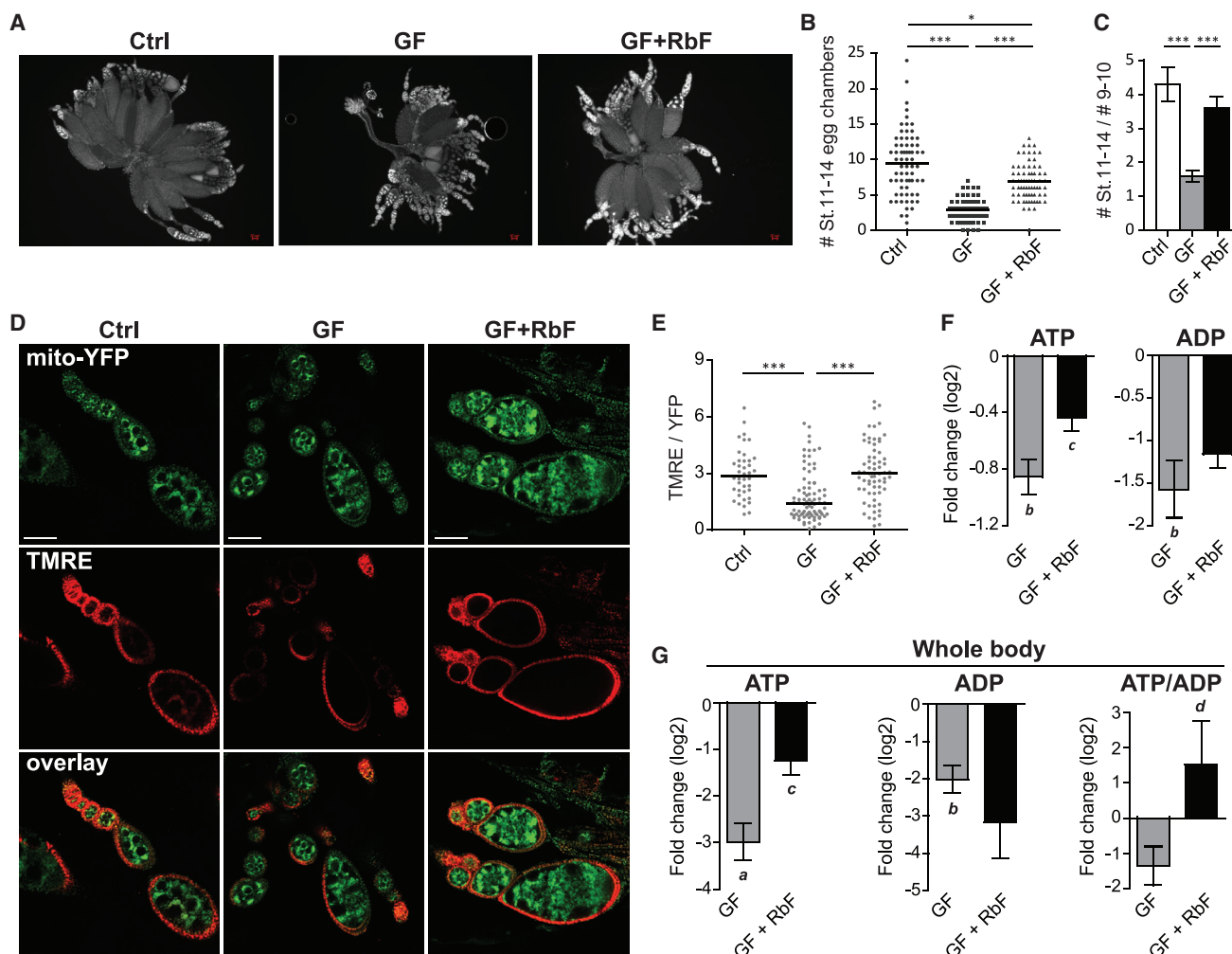


Figure 3. Riboflavin (RbF) Increases Oogenesis and Mitochondrial Function in Follicle Cells of GF Females

(A) Representative images of DAPI-stained ovaries of conventionally raised (Ctrl) and GF OrR females (day 6), with and without RbF supplementation (GF+RbF and GF, respectively). Scale bar, 50 μ m.

(B and C) Number of stage 11–14 egg chambers in ovary (B) and ratio between the numbers in stages 11–14 and 9–10 (C) for the cases in (A). Mean \pm SEM based on 3 independent experiments with $n > 20$ ovaries each; * $p < 0.05$, *** $p < 0.001$ (Kruskal-Wallis with Dunn's multiple comparisons test).

(D and E) Representative images of TMRE-stained ovarioles in day-6 mito-EYFP females (D) and the respective TMRE/EYFP ratio in follicle cells at stages 6–8 (E). Medians of 3 independent experiments; $n > 40$ eggs per condition; *** $p < 0.001$ (Kruskal-Wallis with Dunn's multiple comparisons test). Scale bar, 50 μ m.

(F) ATP and ADP FC (log2) in ovaries of GF females with and without RbF supplementation (GF+RbF and GF, respectively) versus Ctrl. Mean \pm SEM; $n = 9$ with 10 ovaries per sample.

(G) Same as (F) for ATP and ADP and their ratio (ATP/ADP) in the female's whole body (Wb). Means \pm SE; $n = 4$ –5 with 50 females per sample.

a and b, significance versus Ctrl ($p < 0.001$ and $p < 0.01$, respectively); c and d, significance versus GF ($p < 0.01$ and $p < 0.05$, respectively), ANOVA with Tukey's multiple comparisons test.

of 3 metabolites that are degraded by FAD-dependent enzymes (Depeint et al., 2006): pyruvate, succinate, and α -ketoglutarate (Figures 4E and 4F). Analysis of metabolite levels as a function of average female weight in each sample revealed a nearly linear relation between female weight and whole-body levels of ATP and GTP (Figures 4G and S6D).

Based on the degree of similarity of metabolite abundance profiles, hierarchical clustering analysis was performed to show the global overview of all culture supernatant metabolites detected (Fig. 3). Metabolites with similar abundance patterns

were positioned closer together. In addition to these impacts on energy production pathways, removal of gut microbiota increased the amino acids levels in the whole body, but not in ovaries of GF females (Figure 4H). This increase was significantly more pronounced in essential (compared to non-essential) amino acids (Figures 4H and 4I).

Analysis of lipid metabolites revealed a global trend toward higher levels in whole body (but not ovary) of GF females versus controls (Figure 5A). Higher levels were observed in most of the fatty acids (Figure 5B), glycerol derivatives (Figure 5C),

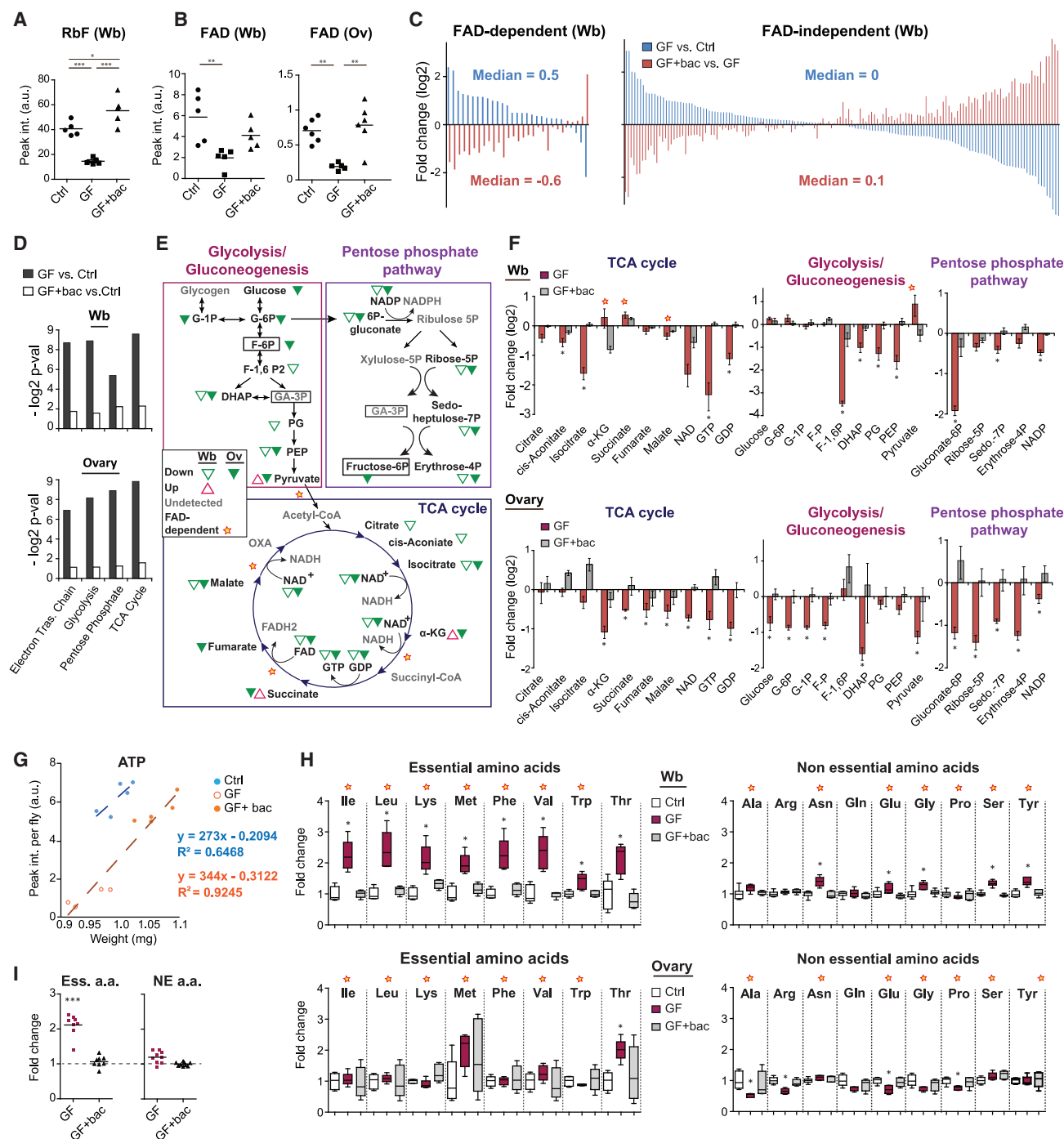


Figure 4. GF Females Have Lower Levels of Metabolites Required for ATP Production

(A) Relative levels of RbF in Wb of day 6 conventionally raised (Ctrl) females and GF females with and without supplementation of native gut bacteria (GF+bac and GF, respectively). $n = 5$ independent measurements (dots), each based on ~50 females.

(B) Same as (A) for levels of flavin adenine dinucleotide (FAD) in Wb and ovaries. $n = 5-6$. * $p < 0.05$, ** $p < 0.01$, *** $p < 0.001$ (ANOVA with Tukey's multiple comparisons test).

(C) Mean FCs (log2) of polar metabolites which are degraded (or modified) by FAD-dependent (left) and FAD-independent enzymes (right). blue, change in GF versus Ctrl; red, change in GF+bac versus GF; $n = 5$ with ~50 females per sample.

(D) Estimated likelihood that the reduced levels of metabolites within the indicated pathways were observed by chance (in Wb and ovaries of GF and GF+bac versus control females). Significance ($-\log_2$ of p value) was estimated by random permutations. See also Figure S6B.

(legend continued on next page)

triglycerides with more than 54 carbons, and lysophosphatidylcholines (lysoPCs) and lysophosphatidylethanolamines (lysoPEs) with 16 and 18 carbons (Figure 5D). The increase in these lysoPCs and lysoPEs was accompanied by consistent decrease of their respective precursors, phosphatidylcholines (PCs), and phosphatidylethanolamines (PEs).

RbF Supplementation Opposes the Increase of Amino Acids and Lipids in GF Females

Because many of the metabolites that were higher in GF females (e.g., pyruvate, α -ketoglutarate, glycerol-3P amino acids, and fatty acids) are known to be degraded by FAD-dependent enzymes, their increase in GF females might be caused by the deficiency of FAD (Figure 4B). Higher levels of these metabolites may also increase the levels of related metabolites that are not directly degraded by FAD-dependent enzymes (e.g., TAGs, glycerol, and DHA) (Figures 5C and 5D). To test this hypothesis, we supplemented the diet of GF females with RbF (FMN/FAD precursor) and tested its ability to counteract the increase of FAD-dependent metabolites. Consistent with this expectation, RbF supplementation led to specific decrease of metabolites that are degraded (or chemically modified) by FMN/FAD-dependent enzymes (Figure 6A, top panel). This includes a widespread decrease in amino acids, TCA metabolites, and glycerol derivatives (Figure 6A, middle and bottom panels). Taken together with the decreased levels of fatty acids and suspected TAGs, lysoPEs, and lysoPCs (Figures 6B and 6C), these findings support a causal contribution of FAD shortage to the increased levels of these metabolites in whole body of GF females.

Connection between Mitochondrial and *Aldh* Influences on Oogenesis

Previous work showed that oogenesis also depends on ovarian activity of *aldehyde dehydrogenase (Aldh)* that was found to be lower in GF females (Elgart et al., 2016). *Aldh* is also known to detoxify reactive aldehyde products of peroxidation in the mitochondria (Chakraborty and Fry, 2011). It raises the possibility that the decrease of *Aldh* in the ovary of GF females might be connected to the reduced mitochondrial function in these females. To evaluate this possibility, we investigated interactions between *Aldh* and mitochondrial function. Inhibition of the mitochondria by exposure to 25 μ M of rotenone from days 3–6 mimicked the repressive impact of bacterial removal on *Aldh* expression in the ovary (Figure S7A). Reciprocal treatment with 3 mM of the *Aldh* inhibitor, cyanamide, phenocopied the tissue-specific impact of bacterial removal on the TMRE/EYFP ratio in developing egg chambers (Figure S7B) and reduced the levels of

ATP and ADP in the ovary (Figure S7C). These results suggest that the reduced mitochondrial function in GF females leads to downregulation of ovarian *Aldh*, which in turn has a negative impact on the mitochondrial function and output in the ovary.

DISCUSSION

Regulation of Host Energy and Oogenesis by Bacterial Influence on Mitochondrial Function

Previous work showed that loss of gut bacteria can repress oogenesis and fecundity (Elgart et al., 2016), but the mechanistic flow of influence from gut to ovary remained uncharacterized. Our findings support a systemic axis of influence, mediated by reduced levels of bacterial-derived RbF and possibly other B vitamins that are required for mitochondrial function but are not synthesized by the host. The reduced levels of RbF in GF hosts were consistent with decreased levels of the RbF derivative, FAD, lower whole-body levels of TCA metabolites, and overall reduction of mitochondrial production and ATP levels in the host. These effects were accompanied by a more pronounced reduction of mitochondrial activity in the ovarian follicle cells and decreased production of late-stage oocytes, resulting in reduced expenditure of energy on reproduction. Supplementation of RbF increased the ATP levels in the whole-body and ovary, restored normal mitochondrial function in the ovarian follicle cells, and increased the number and fraction of late-stage oocytes. Causal contribution of reduced mitochondrial function to the repression of oogenesis was demonstrated in conventionally raised flies by low dosage treatment with rotenone as well by tissue-specific knockdown of key mitochondrial genes in follicle cells. The outcomes of reducing the mitochondrial function were qualitatively and quantitatively comparable to those of removing the gut bacteria. This was demonstrated, for example, by significant correlations between bacterial removal and rotenone treatment with respect to: (1) stage-specific reduction of mitochondrial membrane potential in follicle cells, and (2) changes in mitochondrial gene transcripts in the ovary. These findings show that the removal of gut bacteria decreased the mitochondrial function in the host, and the decreased mitochondrial activity in the ovarian follicle cells suffices to account for the repressed oogenesis.

The reduced mitochondrial function and oogenesis in GF females were largely reversed by RbF complementation, demonstrating a dependence of oogenesis on a bacterial-derived coenzyme that is universally required for mitochondrial function. As a systemic source of FAD (and FMN), RbF may have direct and indirect impacts on oogenesis, mediated

(E) Metabolic diagram of metabolites in the TCA cycle, glycolysis, and pentose phosphate pathways. Metabolites that increase or decrease in Wb and ovaries of GF females versus Ctrl are marked by corresponding triangles (legend box).

(F) FC (log2) of the metabolites in (E). Mean \pm SEM; *false discovery rate (FDR) < 0.05 for GF versus Ctrl (ANOVA with Tukey's multiple comparisons test). stars, FAD (or FMN)-dependent processes.

(G) Wb levels of ATP plotted against female weight for the cases in (A).

(H) FC of essential (left) and non-essential amino acids (right), measured in Wb (upper panel) and ovary (lower panel) by liquid chromatography-mass spectrometry (LC-MS) for the cases in (A). Median \pm quartiles; n = 5–6 with ~50 females/ovaries per sample; *FDR < 0.05 for GF versus Ctrl (ANOVA with Tukey's multiple comparisons test).

(I) FCs of essential (Ess. aa) and non-essential amino acids (NE. aa) in Wb of GF+bac and GF females (both versus Ctrl). Each dot displays average fold-change (n = 5) of a specific amino acid. ***p < 0.001 (ANOVA with Tukey's multiple comparisons test).

See also Figures S4, S5, and S6.

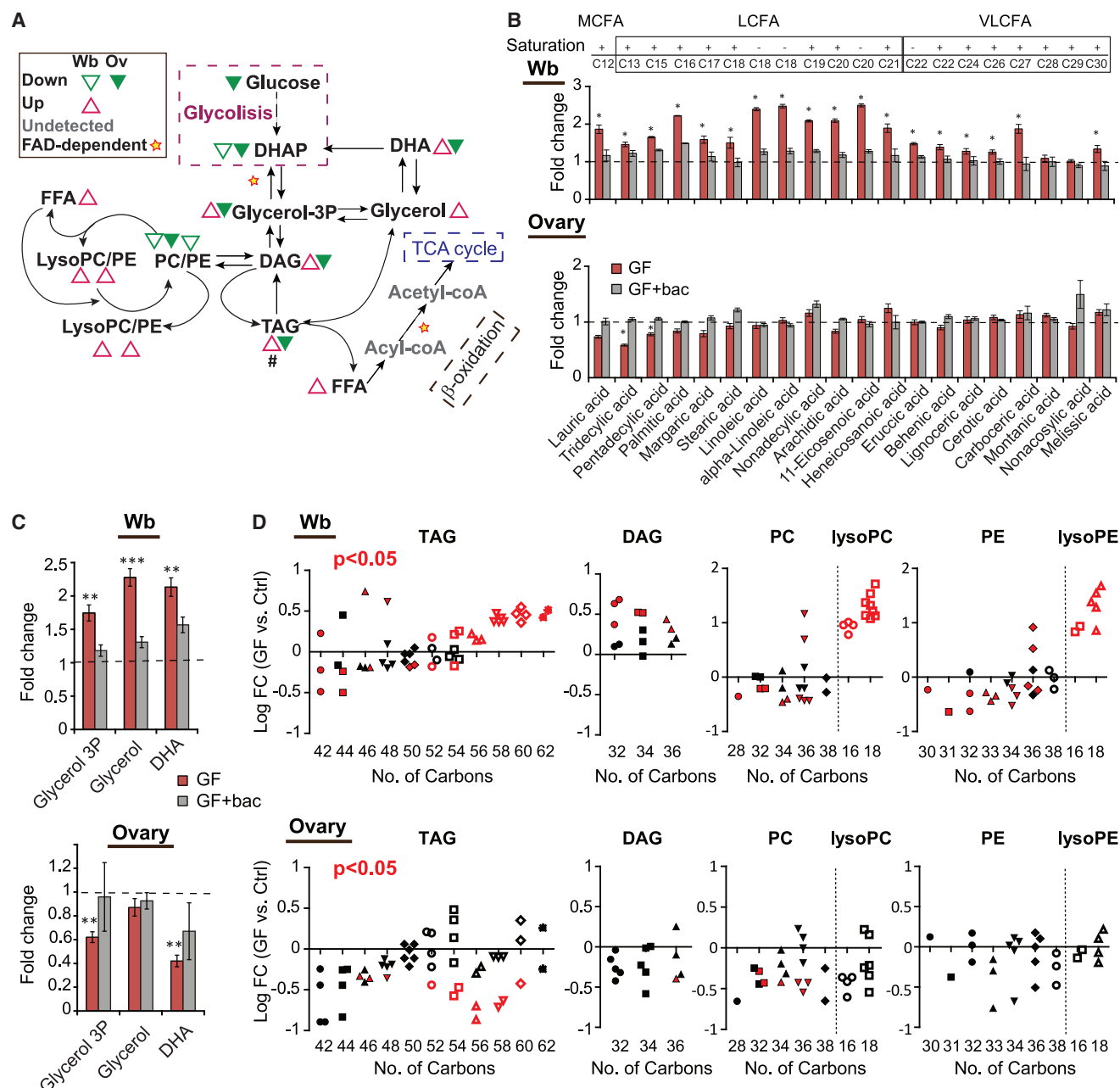


Figure 5. Increased Levels of Lipids in Wb of GF Females

(A) Metabolic diagram of connections between various lipids, indicating significant changes (triangles) in Wb and ovaries of GF versus conventionally raised (Ctrl) females at day 6 (FDR <0.05). stars, FAD (or FMN)-dependent processes. #, indicates upregulation of TAGs with 56 or more carbons.

(B) FCs (log2 versus Ctrl) of specific fatty acids in Wb and ovary of 6-day GF females with and without supplementation of native gut bacteria (GF+bac and GF, respectively). Mean \pm SEM, $n \geq 5$ biological replicates with ~ 50 females/ovary per sample; '+' and '-' signs, saturated and unsaturated fatty acids, respectively; MCFA, medium chain fatty acids; LCFA, long chain fatty acids; VLCFA, very long chain fatty acids.

(C) FC of glycerol derivatives in Wb and ovaries for the cases in (B).

(D) Mean fold-changes (log2) of TAGs, PCs, PEs, lysoPCs, and lysoPEs in Wb (top) and ovaries (bottom). Dots in each carbon group correspond to lipids that have the same number of carbons and different numbers of carbon double bonds. $n = 4-6$ with ~ 50 females/ovaries each sample. red, lipids with significant fold-change; DHA, dihydroxyacetone; TAG, triglycerides; PC, phosphatidylcholine; PE, phosphatidylethanolamine.

*FDR <0.05 (ANOVA with Tukey's multiple comparisons test).

See also Figures S4 and S5.

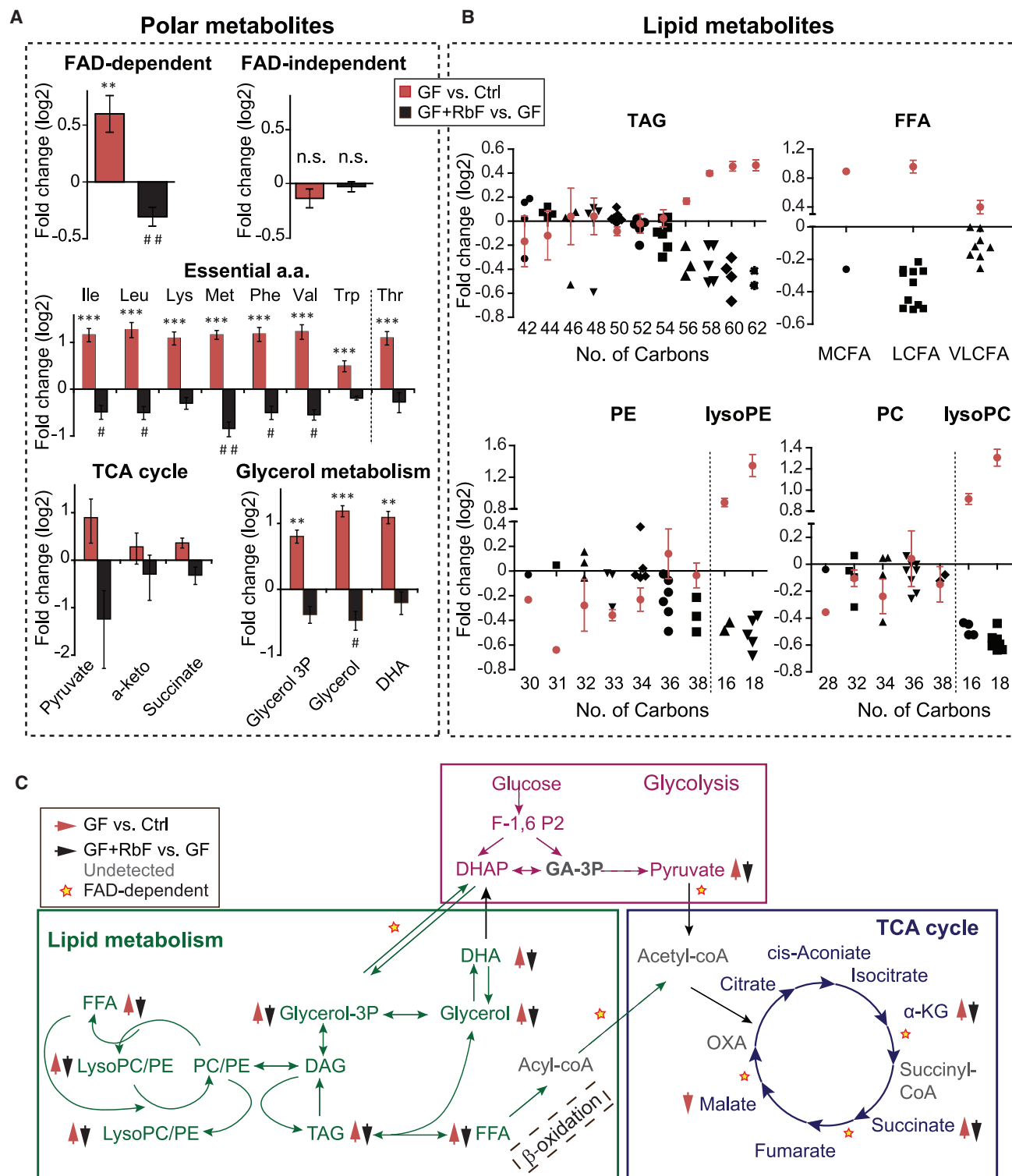


Figure 6. Exogenous RbF Opposes the Increase of FAD-Dependent Metabolites in GF Females

(A) Top: mean FC (log2) of FAD-dependent (left) and FAD-independent polar metabolites (right) analyzed by LC-MS in Wb of females at day 6. red, changes in GF versus control; black, changes in GF with RbF supplementation (GF+RbF) versus GF. Middle: same for essential amino acids. Bottom: same for selected TCA cycle metabolites and glycerol derivatives. Mean \pm SEM; n = 4–5 with \sim 50 females per sample. *p < 0.05, **p < 0.01, and ***p < 0.001 correspond to changes versus Ctrl (t test); #p < 0.05 and ##p < 0.01 correspond to changes versus GF (t test).

(legend continued on next page)

respectively, by local influence of RbF on the mitochondrial function in follicle cells and broader influence on the physiological response to energy status. In either case, the modulation of oogenesis by bacterial-derived RbF does not exclude potential regulation by additional bacterial factors. Involvement of other bacterial factors is, in fact, supported by the more effective (and comprehensive) metabolic restoration achieved by bacterial complementation, versus RbF supplementation alone. Prime candidates for other bacterial factors that may affect the host mitochondria and reproductive function include the B vitamins: B1, thiamin; B3, niacin (NADH precursor); B5, pantothenic acid; B6, pyridoxine; and B7, biotin (Depeint et al., 2006).

Bacterial Influence on Host Amino Acids and Lipids

Although most of the metabolites involved in energy production were lower in GF females, we detected a few notable exceptions, such as increased levels of α -ketoglutarate, succinate, and pyruvate. Because these metabolites are degraded by FAD-dependent enzymes (Zaman and Verwilghen, 1975), their increased levels in GF females might be caused by the deficiency of FAD. A similar rationale may apply to additional metabolites that are degraded by FAD/FMN-dependent enzymes (Kohlmeier, 2015; Lienhart et al., 2013) and potentially also to reactants that are indirectly affected by changes in either the substrates or products of FAD/FMN-dependent enzymes. Direct impact of FAD deficiency may account for the increased whole-body levels of amino acids, purine metabolites, fatty acids, and glycerol-3P (Kohlmeier, 2015). Elevated levels of glycerol-3P and fatty acids may affect related metabolic flows, leading to indirect increase in TAGs, lysoPC/PE, DHA, and glycerol. This is consistent with reported increase of TAGs and fatty acids under loss-of-function of long chain β -oxidation (Kishita et al., 2012) and impairment in catabolism following inhibition of mitochondrial function by knockout of Srt4 (Wood et al., 2018). The restoring impact of RbF supplementation on most of the metabolites that were elevated in GF females further provided detailed functional evidence that the increase in the levels of these metabolites is caused by the depletion of FAD.

Although the shortage of FAD can provide a direct mechanism for the elevated levels of amino acids in GF females, it is not by itself sufficient to explain the more pronounced increase in essential (versus non-essential) amino acids. Yet, the preferential increase of essential amino acids can potentially be explained by combining more uniform increase in amino acids with inability to reduce the synthesis of the essential (but not non-essential) amino acids. Under GF conditions that compromise the production of ATP, the females may benefit from reducing the synthesis of amino acids, but this is only possible for non-essential amino acids. Thus, the lower levels of non-essential amino acids may be due to a compensatory reduction of synthesis that is restricted to these amino acids.

A Unifying Mechanism for Bacterial Involvement in Growth Signaling

Systemic bacterial contribution to mitochondrial function and energy balance in the host may provide explanatory insights on diverse findings in previous studies. *Drosophila* gut bacteria has been shown to increase oxygen consumption (Ridley et al., 2012) and promote larval growth by modulating the insulin signaling pathway (Shin et al., 2011) and TOR nutrient sensing (Storelli et al., 2011). Bacterial independent studies show that ATP and other mitochondrial factors participate in coupling glucose metabolism to insulin secretion (Mattila and Hietakangas, 2017). Uptake of glucose in adult flies stimulates ATP production which, in turn, promotes exocytosis of insulin-like peptides (dILPs) from insulin precursor cells (IPCs) (Park et al., 2014). Conversely, suppression of ATP was shown to inhibit ILP secretion (McCommis et al., 2016), and uncoupling of mitochondrial activity in *Drosophila* neurons led to repression of insulin signaling (Fridell et al., 2009). Genetic analyses in flies further identified the *Drosophila* TOR (dTOR) as a downstream effector of the insulin pathway (Hay and Sonenberg, 2004; Kim and Neufeld, 2015). Similar connections between insulin, TOR, and mitochondrial function were reported in mammals (Hay and Sonenberg, 2004; Troulinaki and Bano, 2012). The current findings of the bacterial influence on mitochondrial function and ATP production offer a simple unifying mechanism, explaining how gut bacteria can modulate the insulin and TOR pathways in diverse species and how fecundity is regulated by both insulin (Das and Arur, 2017; Sieber et al., 2016) and bacteria (Elgart et al., 2016).

Systemic versus Local Regulation by Gut Bacteria

It was previously shown that gut bacteria can support oogenesis by promoting *Aldh* activity in the ovary (Elgart et al., 2016), but the flow of influence from gut to ovary was not investigated. The bacterial-mitochondrial connection may fill this influence gap directly and/or indirectly. These include local influence of bacterial-derived B-vitamins on mitochondrial activity in somatic follicle cells that provide essential metabolites to developing oocytes (Sieber and Spradling, 2017; Spradling, 1993) and global, signaling-based repression of oogenesis that may be needed to secure enough ATP for essential functions. Evaluating relative contributions of local and global bacterial influences on oogenesis is confounded by the pleiotropic functions of bacterial-derived vitamins. For example, the positive effect of RbF on oogenesis in GF flies may be caused by local influence of RbF on ovarian follicle cells or by a signaling pathway that promotes physiological upregulation of oogenesis. A combined scenario is also plausible and is supported, to some extent, by the finding that exogenous RbF restored the mitochondrial membrane potential in the follicle cells of GF females, but the ATP levels were only partially restored.

(B) FC (log2) of various lipid metabolites. Each dot corresponds to the average change in a group of medium, long, and very long chain fatty acids (top right) and in sets of TAGs, PCs, lysoPCs, PEs, and lysoPEs with a given number of carbons (top left, bottom left, and right). $n = 4-5$ (~50 females per sample).

(C) Metabolic diagram with indicators (arrows) for the opposite impacts of bacterial removal (red) and RbF supplementation (black) on TCA, glycolysis, and lipid metabolites that are degraded (or potentially affected) by FAD-dependent enzymes. stars, FAD (or FMN)-dependent processes; DHA, dihydroxyacetone; TAG, triglycerides; PC, phosphatidylcholine; PE, phosphatidylethanolamine.

Conservation of the Bacterial-Mitochondrial Axis of Regulating Host Energy and Oogenesis

The high conservation of biochemical reactions involved in energy production and their reliance on a small number of signaling pathway (Das and Arur, 2017; Hay and Sonenberg, 2004; Ikeya et al., 2002), suggest that the bacterial-mitochondrial axis also regulates host growth and fecundity in mammals. This is supported by multiple lines of evidence in mice and human. In line with our *Drosophila* findings, the level of insulin in the plasma of GF mice was lower compared to control mice (Rabot et al., 2010), and the serum of GF mice had lower levels of citrate, fumarate, and malate and higher levels of linoleic and palmitic acids (Velagapudi et al., 2010). GF mice also exhibited similar patterns of increase in amino acids and large TAGs and decrease in phosphatidylcholines with 34–38 carbons (Mardinoglu et al., 2015; Velagapudi et al., 2010). The similarity between the impacts of gut bacteria on energy production pathways in flies and mammals likely reflects the highly conserved influence of mitochondrial coenzymes that are derived from bacterial vitamins. The proposed contribution of bacterial factors to energy production in the host is also consistent with recent estimation of bacterial contribution to heat production in human (Rosenberg and Zilber-Rosenberg, 2016).

Comparing our findings with mitochondrial effects on oogenesis in species with substantially different anatomy of reproduction (Babayev and Seli, 2015; Cecchino et al., 2018; Copeland et al., 2009) suggests that the regulation of oogenesis by a bacterial-mitochondrial connection is also conserved. Mitochondrial activity in mammals, for example, is essential for oocyte maturation, fertilization, and embryonic development (Babayev and Seli, 2015; Cecchino et al., 2018). Mitochondrial dysfunction, along with unbalanced levels of glucose and high TAG and fatty acid levels, was associated with meiotic defects (Wu et al., 2010) and delayed development of murine oocytes (Wang et al., 2010). Similarly to oogenesis in flies, the development of mammalian oocytes depends on adjacent somatic granulosa cumulus cells that surround the oocyte in the ovarian follicle (Gilchrist et al., 2008; Thompson et al., 2007) and provides it with carbohydrates, lipids, amino acids, and ATP (Buccione et al., 1990; Dumesic et al., 2015). The follicular microenvironment is also a dominant factor in oocyte developmental potential in human (Fauser et al., 2011), and the analysis of cumulus cells is considered a preferred non-invasive strategy for evaluating oocyte competence and quality (Boucret et al., 2015; Desquiere-Dumas et al., 2017; Dumesic et al., 2015). This evidence supports a conserved contribution of mitochondrial follicle function to oogenesis within the follicle tissue. Taken together with conservation of insulin signaling, nutrient sensing, and mitochondrial co-factors, our findings provide strong support for a conserved bacterial-mitochondrial axis, regulating host energy production and oogenesis.

STAR★METHODS

Detailed methods are provided in the online version of this paper and include the following:

● KEY RESOURCES TABLE

● RESOURCE AVAILABILITY

- Lead Contact
- Materials Availability
- Data and Code Availability

● EXPERIMENTAL MODEL AND SUBJECT DETAILS

- *Drosophila* strains and diet

● METHOD DETAILS

- Bacterial removal and re-colonization
- DAPI staining and ovary staging
- Mitochondrial DNA quantification
- Quantitative RT-PCR
- ATP and ADP analysis by quantitative LC-MS/MS
- Measurements of mitochondrial membrane potential
- RNAi experiments
- Efficiency of RNAi inhibition test
- Metabolomics and Lipidomics
- Lipidomics analysis
- Analysis of polar metabolites
- Metabolite identification

● QUANTIFICATION AND STATISTICAL ANALYSIS

- Metabolic statistical analysis
- Permutation analysis

SUPPLEMENTAL INFORMATION

Supplemental Information can be found online at <https://doi.org/10.1016/j.celrep.2020.108583>.

ACKNOWLEDGMENTS

We thank Vladimir Kiss and Dr. Reinat Nevo (Weizmann Institute of Science) for intellectual and technical assistance in image analysis. We thank Prof. Michael Walker (Weizmann Institute of Science) and Dr. Yael Heifetz (Hebrew University) for helpful discussions and suggestions, and Maiar Ibrahim and Yael Hanoch for technical and experimental assistance. We also thank the Weizmann Fly's core facility for providing technical support and Weizmann Design Brunch for graphical abstract design assistance. This work was supported by the Sir John Templeton Foundation (40663 and 61122). The work of S.M. and M.I. was supported by the Vera and John Schwartz Family Center for Metabolic Biology.

AUTHOR CONTRIBUTIONS

Y.G. and Y.S. designed and supervised the study and wrote the paper. Y.G., N.Z., M.E., and E.O. performed experiments and data analysis. A.B. and T.M. performed targeted measurements of ATP and ADP. S.M. and M.I. performed targeted metabolomics and lipidomics analysis. J.A. performed the initial metabolomics measurements.

DECLARATION OF INTERESTS

The authors declare no competing interests.

Received: July 23, 2019
Revised: October 2, 2020
Accepted: December 10, 2020
Published: January 5, 2021

REFERENCES

- Babayev, E., and Seli, E. (2015). Oocyte mitochondrial function and reproduction. *Curr. Opin. Obstet. Gynecol.* 27, 175–181.
- Bafunno, V., Giancaspero, T.A., Brizio, C., Bufano, D., Passarella, S., Boles, E., and Barile, M. (2004). Riboflavin uptake and FAD synthesis in *Saccharomyces*

cerevisiae mitochondria: involvement of the Flx1p carrier in FAD export. *J. Biol. Chem.* 279, 95–102.

Boucret, L., Chao de la Barca, J.M., Morinière, C., Desquret, V., Ferré-L'Hôtelier, V., Descamps, P., Marcaillou, C., Reynier, P., Procaccio, V., and May-Panloup, P. (2015). Relationship between diminished ovarian reserve and mitochondrial biogenesis in cumulus cells. *Hum. Reprod.* 30, 1653–1664.

Broderick, N.A., Buchon, N., and Lemaitre, B. (2014). Microbiota-induced changes in *Drosophila melanogaster* host gene expression and gut morphology. *MBio* 5, e01117–e14.

Brummel, T., Ching, A., Seroude, L., Simon, A.F., and Benzer, S. (2004). *Drosophila* lifespan enhancement by exogenous bacteria. *Proc. Natl. Acad. Sci. USA* 101, 12974–12979.

Buccione, R., Schroeder, A.C., and Eppig, J.J. (1990). Interactions between somatic cells and germ cells throughout mammalian oogenesis. *Biol. Reprod.* 43, 543–547.

Buchon, N., Broderick, N.A., Chakrabarti, S., and Lemaitre, B. (2009a). Invasive and indigenous microbiota impact intestinal stem cell activity through multiple pathways in *Drosophila*. *Genes Dev.* 23, 2333–2344.

Buchon, N., Broderick, N.A., Poidevin, M., Pradervand, S., and Lemaitre, B. (2009b). *Drosophila* intestinal response to bacterial infection: activation of host defense and stem cell proliferation. *Cell Host Microbe* 5, 200–211.

Cecchino, G.N., Seli, E., Alves da Motta, E.L., and García-Velasco, J.A. (2018). The role of mitochondrial activity in female fertility and assisted reproductive technologies: overview and current insights. *Reprod. Biomed. Online* 36, 686–697.

Chakraborty, M., and Fry, J.D. (2011). *Drosophila* lacking a homologue of mammalian ALDH2 have multiple fitness defects. *Chem. Biol. Interact.* 191, 296–302.

Chappel, S. (2013). The role of mitochondria from mature oocyte to viable blastocyst. *Obstet. Gynecol. Int.* 2013, 183024.

Chong, J., Soufan, O., Li, C., Caraus, I., Li, S., Bourque, G., Wishart, D.S., and Xia, J. (2018). MetaboAnalyst 4.0: towards more transparent and integrative metabolomics analysis. *Nucleic Acids Res.* 46 (W1), W486–W494.

Copeland, J.M., Cho, J., Lo, T., Jr., Hur, J.H., Bahadorani, S., Arabyan, T., Rabie, J., Soh, J., and Walker, D.W. (2009). Extension of *Drosophila* life span by RNAi of the mitochondrial respiratory chain. *Curr. Biol.* 19, 1591–1598.

Das, D., and Arur, S. (2017). Conserved insulin signaling in the regulation of oocyte growth, development, and maturation. *Mol. Reprod. Dev.* 84, 444–459.

Depeint, F., Bruce, W.R., Shangari, N., Mehta, R., and O'Brien, P.J. (2006). Mitochondrial function and toxicity: role of B vitamins on the one-carbon transfer pathways. *Chem. Biol. Interact.* 163, 113–132.

Desquret-Dumas, V., Clément, A., Seegers, V., Boucret, L., Ferré-L'Hôtelier, V., Bouet, P.E., Descamps, P., Procaccio, V., Reynier, P., and May-Panloup, P. (2017). The mitochondrial DNA content of cumulus granulosa cells is linked to embryo quality. *Hum. Reprod.* 32, 607–614.

Drummond-Barbosa, D., and Spradling, A.C. (2001). Stem cells and their progeny respond to nutritional changes during *Drosophila* oogenesis. *Dev. Biol.* 231, 265–278.

Dumesic, D.A., Meldrum, D.R., Katz-Jaffe, M.G., Krisner, R.L., and Schoolcraft, W.B. (2015). Oocyte environment: follicular fluid and cumulus cells are critical for oocyte health. *Fertil. Steril.* 103, 303–316.

Elgart, M., and Soen, Y. (2018). Microbiome-Germline Interactions and Their Transgenerational Implications. *Bioessays* 40, 1700018.

Elgart, M., Stern, S., Salton, O., Gnainsky, Y., Heifetz, Y., and Soen, Y. (2016). Impact of gut microbiota on the fly's germ line. *Nat. Commun.* 7, 11280.

Fausser, B.C., Diedrich, K., Bouchard, P., Domínguez, F., Matzuk, M., Franks, S., Hamamah, S., Simón, C., Devroey, P., Ezcurra, D., and Howles, C.M.; Evian Annual Reproduction (EVAR) Workshop Group 2010 (2011). Contemporary genetic technologies and female reproduction. *Hum. Reprod. Update* 17, 829–847.

Fischer, C.N., Trautman, E.P., Crawford, J.M., Stabb, E.V., Handelsman, J., and Broderick, N.A. (2017). Metabolite exchange between microbiome mem-

bers produces compounds that influence *Drosophila* behavior. *eLife* 6, e18855.

Fridell, Y.W., Hoh, M., Kréneisz, O., Hosier, S., Chang, C., Scantling, D., Mulkey, D.K., and Helfand, S.L. (2009). Increased uncoupling protein (UCP) activity in *Drosophila* insulin-producing neurons attenuates insulin signaling and extends lifespan. *Aging (Albany NY)* 1, 699–713.

Fridmann-Sirkis, Y., Stern, S., Elgart, M., Galili, M., Zeisel, A., Shental, N., and Soen, Y. (2014). Delayed development induced by toxicity to the host can be inherited by a bacterial-dependent, transgenerational effect. *Front. Genet.* 5, 27.

Gilchrist, R.B., Lane, M., and Thompson, J.G. (2008). Oocyte-secreted factors: regulators of cumulus cell function and oocyte quality. *Hum. Reprod. Update* 14, 159–177.

Hansen, M., Flatt, T., and Aguilaniu, H. (2013). Reproduction, fat metabolism, and life span: what is the connection? *Cell Metab.* 17, 10–19.

Hay, N., and Sonenberg, N. (2004). Upstream and downstream of mTOR. *Genes Dev.* 18, 1926–1945.

Henriques, S.F., Dhakan, D.B., Serra, L., Francisco, A.P., Carvalho-Santos, Z., Baltazar, C., Elias, A.P., Anjos, M., Zhang, T., Maddocks, O.D.K., and Ribeiro, C. (2020). Metabolic cross-feeding in imbalanced diets allows gut microbes to improve reproduction and alter host behaviour. *Nat. Commun.* 11, 4236.

Ikeya, T., Galic, M., Belawat, P., Nairz, K., and Hafen, E. (2002). Nutrient-dependent expression of insulin-like peptides from neuroendocrine cells in the CNS contributes to growth regulation in *Drosophila*. *Curr. Biol.* 12, 1293–1300.

Keebaugh, E.S., Yamada, R., Obadia, B., Ludington, W.B., and Ja, W.W. (2018). Microbial Quantity Impacts *Drosophila* Nutrition, Development, and Lifespan. *iScience* 4, 247–259.

Kim, J., and Neufeld, T.P. (2015). Dietary sugar promotes systemic TOR activation in *Drosophila* through AKH-dependent selective secretion of Dilp3. *Nat. Commun.* 6, 6846.

Kishita, Y., Tsuda, M., and Aigaki, T. (2012). Impaired fatty acid oxidation in a *Drosophila* model of mitochondrial trifunctional protein (MTP) deficiency. *Biochem. Biophys. Res. Commun.* 419, 344–349.

Kohlmeier, M. (2015). Water-soluble vitamins and nonnutrients. *Nutrient Metabolism: Structures, Functions, and Genes* (Academic Press), pp. 589–599.

LeBlanc, J.G., Milani, C., de Giori, G.S., Sesma, F., van Sinderen, D., and Ventura, M. (2013). Bacteria as vitamin suppliers to their host: a gut microbiota perspective. *Curr. Opin. Biotechnol.* 24, 160–168.

Lee, J.S., Adler, L., Karathia, H., Carmel, N., Rabinovich, S., Auslander, N., Keshet, R., Stettner, N., Silberman, A., Agemy, L., et al. (2018). Urea Cycle Dysregulation Generates Clinically Relevant Genomic and Biochemical Signatures. *Cell* 174, 1559–1570.

Leitão-Gonçalves, R., Carvalho-Santos, Z., Francisco, A.P., Fioreze, G.T., Anjos, M., Baltazar, C., Elias, A.P., Itskov, P.M., Piper, M.D.W., and Ribeiro, C. (2017). Commensal bacteria and essential amino acids control food choice behavior and reproduction. *PLoS Biol.* 15, e2000862.

Lienhart, W.D., Gudipati, V., and Macheroux, P. (2013). The human flavoproteome. *Arch. Biochem. Biophys.* 535, 150–162.

Malitsky, S., Ziv, C., Rosenwasser, S., Zheng, S., Schatz, D., Porat, Z., Bendor, S., Aharoni, A., and Vardi, A. (2016). Viral infection of the marine alga *Emiliania huxleyi* triggers lipidome remodeling and induces the production of highly saturated triacylglycerol. *New Phytol.* 210, 88–96.

Mardinoglu, A., Shoaie, S., Bergentall, M., Ghaffari, P., Zhang, C., Larsson, E., Bäckhed, F., and Nielsen, J. (2015). The gut microbiota modulates host amino acid and glutathione metabolism in mice. *Mol. Syst. Biol.* 11, 834.

Mattila, J., and Hietakangas, V. (2017). Regulation of Carbohydrate Energy Metabolism in *Drosophila melanogaster*. *Genetics* 207, 1231–1253.

May-Panloup, P., Boucret, L., Chao de la Barca, J.M., Desquret-Dumas, V., Ferré-L'Hôtelier, V., Morinière, C., Descamps, P., Procaccio, V., and Reynier, P. (2016). Ovarian ageing: the role of mitochondria in oocytes and follicles. *Hum. Reprod. Update* 22, 725–743.

- McCommis, K.S., Hodges, W.T., Bricker, D.K., Wisidagama, D.R., Compan, V., Remedi, M.S., Thummel, C.S., and Finck, B.N. (2016). An ancestral role for the mitochondrial pyruvate carrier in glucose-stimulated insulin secretion. *Mol. Metab.* **5**, 602–614.
- Min, K.J., and Tatar, M. (2018). Unraveling the Molecular Mechanism of Immunosenescence in *Drosophila*. *Int. J. Mol. Sci.* **19**, 2472.
- Morimoto, J., Simpson, S.J., and Ponton, F. (2017). Direct and trans-generational effects of male and female gut microbiota in *Drosophila melanogaster*. *Biol. Lett.* **13**, 20160966.
- Neis, E.P., Dejong, C.H., and Rensen, S.S. (2015). The role of microbial amino acid metabolism in host metabolism. *Nutrients* **7**, 2930–2946.
- Newell, P.D., and Douglas, A.E. (2014). Interspecies interactions determine the impact of the gut microbiota on nutrient allocation in *Drosophila melanogaster*. *Appl. Environ. Microbiol.* **80**, 788–796.
- Nguyen, B., Than, A., Dinh, H., Morimoto, J., and Ponton, F. (2020). Parental Microbiota Modulates Offspring Development, Body Mass and Fecundity in a Polyphagous Fruit Fly. *Microorganisms* **8**, 1289.
- Park, S., Alfa, R.W., Topper, S.M., Kim, G.E., Kockel, L., and Kim, S.K. (2014). A genetic strategy to measure circulating *Drosophila* insulin reveals genes regulating insulin production and secretion. *PLoS Genet.* **10**, e1004555.
- Parker, D.J., Moran, A., and Mitra, K. (2017). Studying Mitochondrial Structure and Function in *Drosophila* Ovaries. *J. Vis. Exp.* (119), 54989.
- Rabot, S., Membrez, M., Bruneau, A., Gérard, P., Harach, T., Moser, M., Raymond, F., Mansourian, R., and Chou, C.J. (2010). Germ-free C57BL/6J mice are resistant to high-fat-diet-induced insulin resistance and have altered cholesterol metabolism. *FASEB J.* **24**, 4948–4959.
- Reedy, A.R., Luo, L., Neish, A.S., and Jones, R.M. (2019). Commensal microbiota-induced redox signaling activates proliferative signals in the intestinal stem cell microenvironment. *Development* **146**, dev171520.
- Ridley, E.V., Wong, A.C., Westmiller, S., and Douglas, A.E. (2012). Impact of the resident microbiota on the nutritional phenotype of *Drosophila melanogaster*. *PLoS ONE* **7**, e36765.
- Rosenberg, E., and Zilber-Rosenberg, I. (2016). Do microbiotas warm their hosts? *Gut Microbes* **7**, 283–285.
- Ryu, J.-H., Kim, S.-H., Lee, H.-Y., Bai, J.-Y., Nam, Y.-D., Bae, J.-W., Lee, D.G., Shin, S.C., Ha, E.-M., and Lee, W.-J. (2008). Innate immune homeostasis by the homeobox gene caudal and commensal-gut mutualism in *Drosophila*. *Science* **319**, 777–782.
- Sannino, D.R., Dobson, A.J., Edwards, K., Angert, E.R., and Buchon, N. (2018). The *Drosophila melanogaster* Gut Microbiota Provisions Thiamine to Its Host. *MBio* **9**, e00155–18.
- Schindelin, J., Arganda-Carreras, I., Frise, E., Kaynig, V., Longair, M., Pietzsch, T., Preibisch, S., Rueden, C., Saalfeld, S., Schmid, B., et al. (2012). Fiji: an open-source platform for biological-image analysis. *Nat. Methods* **9**, 676–682.
- Schretter, C.E., Vielmetter, J., Bartos, I., Marka, Z., Marka, S., Argade, S., and Mazmanian, S.K. (2018). A gut microbial factor modulates locomotor behaviour in *Drosophila*. *Nature* **563**, 402–406.
- Sharon, G., Segal, D., Ringo, J.M., Hefetz, A., Zilber-Rosenberg, I., and Rosenberg, E. (2010). Commensal bacteria play a role in mating preference of *Drosophila melanogaster*. *Proc. Natl. Acad. Sci. USA* **107**, 20051–20056.
- Shin, S.C., Kim, S.-H., You, H., Kim, B., Kim, A.C., Lee, K.-A., Yoon, J.-H., Ryu, J.-H., and Lee, W.-J. (2011). *Drosophila* microbiome modulates host developmental and metabolic homeostasis via insulin signaling. *Science* **334**, 670–674.
- Sieber, M.H., and Spradling, A.C. (2017). The role of metabolic states in development and disease. *Curr. Opin. Genet. Dev.* **45**, 58–68.
- Sieber, M.H., Thomsen, M.B., and Spradling, A.C. (2016). Electron Transport Chain Remodeling by GSK3 during Oogenesis Connects Nutrient State to Reproduction. *Cell* **164**, 420–432.
- Spradling, A.C. (1993). *Developmental Genetics of Oogenesis* Volume U (Cold Spring Harbor Laboratory).
- Storelli, G., Defaye, A., Erkosar, B., Hols, P., Royet, J., and Leulier, F. (2011). *Lactobacillus plantarum* promotes *Drosophila* systemic growth by modulating hormonal signals through TOR-dependent nutrient sensing. *Cell Metab.* **14**, 403–414.
- Terashima, J., Takaki, K., Sakurai, S., and Bownes, M. (2005). Nutritional status affects 20-hydroxyecdysone concentration and progression of oogenesis in *Drosophila melanogaster*. *J. Endocrinol.* **187**, 69–79.
- Thevenon, D., Engel, E., Avet-Rochex, A., Gottar, M., Bergeret, E., Tricoire, H., Benaud, C., Baudier, J., Taillebourg, E., and Fauvarque, M.O. (2009). The *Drosophila* ubiquitin-specific protease dUSP36/Scny targets IMD to prevent constitutive immune signaling. *Cell Host Microbe* **6**, 309–320.
- Thompson, J.G., Lane, M., and Gilchrist, R.B. (2007). Metabolism of the bovine cumulus-oocyte complex and influence on subsequent developmental competence. *Soc. Reprod. Fertil. Suppl.* **64**, 179–190.
- Troulinaki, K., and Bano, D. (2012). Mitochondrial deficiency: a double-edged sword for aging and neurodegeneration. *Front. Genet.* **3**, 244.
- Udhayabalan, T., Manole, A., Rajeshwari, M., Varalakshmi, P., Houlden, H., and Ashokkumar, B. (2017). Riboflavin Responsive Mitochondrial Dysfunction in Neurodegenerative Diseases. *J. Clin. Med.* **6**, 52.
- Velagapudi, V.R., Hezaveh, R., Reigstad, C.S., Gopalacharyulu, P., Yetukuri, L., Islam, S., Felin, J., Perkins, R., Borén, J., Oresic, M., and Bäckhed, F. (2010). The gut microbiota modulates host energy and lipid metabolism in mice. *J. Lipid Res.* **51**, 1101–1112.
- Wang, Q., Frolova, A.I., Purcell, S., Adastra, K., Schoeller, E., Chi, M.M., Schedl, T., and Moley, K.H. (2010). Mitochondrial dysfunction and apoptosis in cumulus cells of type I diabetic mice. *PLoS ONE* **5**, e15901.
- Wong, A.C., Dobson, A.J., and Douglas, A.E. (2014). Gut microbiota dictates the metabolic response of *Drosophila* to diet. *J. Exp. Biol.* **217**, 1894–1901.
- Wong, A.C., Wang, Q.P., Morimoto, J., Senior, A.M., Lihoreau, M., Neely, G.G., Simpson, S.J., and Ponton, F. (2017). Gut Microbiota Modifies Olfactory-Guided Microbial Preferences and Foraging Decisions in *Drosophila*. *Curr. Biol.* **27**, 2397–2404.e4.
- Wood, J.G., Schwer, B., Wickremesinghe, P.C., Hartnett, D.A., Burhenn, L., Garcia, M., Li, M., Verdin, E., and Helfand, S.L. (2018). Sirt4 is a mitochondrial regulator of metabolism and lifespan in *Drosophila melanogaster*. *Proc. Natl. Acad. Sci. USA* **115**, 1564–1569.
- Wu, L.L., Dunning, K.R., Yang, X., Russell, D.L., Lane, M., Norman, R.J., and Robker, R.L. (2010). High-fat diet causes lipotoxicity responses in cumulus-oocyte complexes and decreased fertilization rates. *Endocrinology* **151**, 5438–5445.
- Yamada, R., Deshpande, S.A., Bruce, K.D., Mak, E.M., and Ja, W.W. (2015). Microbes Promote Amino Acid Harvest to Rescue Undernutrition in *Drosophila*. *Cell Rep.* **10**, 865–872.
- Yuval, B. (2017). Symbiosis: Gut Bacteria Manipulate Host Behaviour. *Curr. Biol.* **27**, R746–R747.
- Zaman, Z., and Verwilghen, R.L. (1975). Effects of riboflavin deficiency on oxidative phosphorylation, flavin enzymes and coenzymes in rat liver. *Biochem. Biophys. Res. Commun.* **67**, 1192–1198.
- Zheng, L., Cardaci, S., Jerby, L., MacKenzie, E.D., Sciacovelli, M., Johnson, T.I., Gaude, E., King, A., Leach, J.D., Edrada-Ebel, R., et al. (2015). Fumarate induces redox-dependent senescence by modifying glutathione metabolism. *Nat. Commun.* **6**, 6001.

STAR★METHODS

KEY RESOURCES TABLE

REAGENT or RESOURCE	SOURCE	IDENTIFIER
Bacterial and Virus Strains		
Colony 1 (<i>Acetobacter</i> spp.)	Fridmann-Sirkis et al., 2014	N/A
Chemicals, Peptides, and Recombinant Proteins		
Riboflavin	Sigma-Aldrich	Cat#R4500
Cyanamide	ACROS organics	Cat#181950250
Rotenone	Sigma-Aldrich	Cat#R8875
Formaldehyde solution	Sigma-Aldrich	Cat#F8775
Tetramethyl rhodamine ethyl ester (TMRE)	Sigma-Aldrich	Cat#87917
Critical Commercial Assays		
Vectashield with DAPI	Vector labs	Cat#H-1200
UltraClean tissue and cell DNA isolation kit	Mo Bio labs	Cat#12334-250
Quick-RNA MicroPep kit	Zymo	Cat#R1051
High-Capacity cDNA Reverse Transcription kit	Thermo Fisher Scientific	Cat#4368814
Fast SYBR Green Master mix	Applied Biosystems	Cat#4385614
Experimental Models: Organisms/Strains		
<i>D. melanogaster</i> : yw	Prof. Eli Arama (Weizmann Institute of Science)	N/A
<i>D. melanogaster</i> : OrR	Prof. Adi Salzberg (Technion-Israel Institute of Technology)	N/A
<i>D. melanogaster</i> : UAS-ND-SGDH-RNAi	Vienna Drosophila Resource Center	VDRC: v101385; RRID: FlyBase_FBst0473258
<i>D. melanogaster</i> : UAS-cgnone-RNAi (Ctrl)	Prof. Eli Arama (Weizmann Institute of Science)	VDRC: v103120
<i>D. melanogaster</i> : UAS-ND-20-RNAi	Vienna Drosophila Resource Center	VDRC: v101881; RRID: FlyBase_FBst0473754
<i>D. melanogaster</i> : mito-EYFP w ⁺ ; P{w[+mC] = sqh-EYFP-Mito}3	Bloomington Drosophila Stock Center	BDSC: 7194; RRID: BDSC_7194
<i>D. melanogaster</i> : Nos-Gal4-VP16	Bloomington Drosophila Stock Center	BDSC: 4937; RRID:BDSC_4937
<i>D. melanogaster</i> : Tj-Gal4	Prof. Eli Arama (Weizmann Institute of Science)	N/A
Oligonucleotides		
qPCR Primers	See Table S1	N/A
Software and Algorithms		
Graphpad Prism	GraphPad software	https://www.graphpad.com:443/
Fiji/ImageJ	Schindelin et al., 2012	https://Fiji.sc
UNIFI Version 1.9.2	Waters Corp.	N/A
TraceFinder	Thermo Fisher Scientific	N/A
MetaboAnalyst 4.0	Chong et al., 2018	https://www.metaboanalyst.ca
MATLAB	MathWorks, Inc	https://www.mathworks.com
Other		
ViiA7 Real-Time PCR system	Applied Biosystems	N/A
Confocal Olympus FlowView FV1000	Olympus	N/A
Inverted microscope	Nikon	N/A
qLC-MS/MS	Waters corp.	N/A

(Continued on next page)

Continued

REAGENT or RESOURCE	SOURCE	IDENTIFIER
Aquity I class UPLC System combined with Exactive Plus Orbitrap mass spectrometer	Thermo Fisher Scientific	N/A
Waters ACQUITY UPLC system coupled to a Vion IMS QToF mass spectrometer	Waters corp.	N/A

RESOURCE AVAILABILITY

Lead Contact

Further information and requests for resources and reagents should be directed to and will be fulfilled by the Lead Contact, Yulia Gnainsky (yulia.gnainsky@weizmann.ac.il)

Materials Availability

This study did not generate new unique reagents.

Data and Code Availability

Metabolomics dataset supporting the current study has not been deposited in a public repository because it is still being used in a related ongoing study, but it is available from the corresponding author on request.

EXPERIMENTAL MODEL AND SUBJECT DETAILS

***Drosophila* strains and diet**

Drosophila strains used in this study are listed in the [Key Resources Table](#). Flies were maintained at 25°C on Bloomington standard cornmeal diet with 1.2% yeast (<http://flystocks.bio.indiana.edu/FlyWork/media-recipes/molassesfood.htm>), as described previously ([Elgart et al., 2016](#)). Riboflavin (Sigma), cyanamide (ACROS) and rotenone (Sigma) were added after the food has been cooled to ~50. Experimental procedures are indicated below in [Method Details](#).

METHOD DETAILS

Bacterial removal and re-colonization

Removal of gut bacteria was achieved by dechoriation and sterilization, as described previously ([Elgart et al., 2016](#)). Re-colonization with native bacteria or by mono-association with specific species of gut bacteria were performed, respectively, by overnight placement of five naive males in vials with dechorionated embryos or by food supplementation with *Acetobacter* spp. from *Colony 1* ([Elgart et al., 2016](#); [Fridmann-Sirkis et al., 2014](#)). Flies developed from control (Ctrl), dechorionated (germ-free, GF) and recolonized embryos (GF+bac), were transferred, 0-2 days post-eclosion, to new sterile vials and collected for further analyses at day 6. Bacterial removal and re-colonization were confirmed at the end of every experiment, by inoculating food samples on YPD plates and/or by sequencing of (PCR-amplified) DNA, coding for 16S rRNA ([Elgart et al., 2016](#)).

DAPI staining and ovary staging

Ovaries were dissected in phosphate-buffered saline (PBS), fixed with 4% formaldehyde (Sigma) and mounted using Vectashield mounting medium with DAPI (Vector), as described previously ([Elgart et al., 2016](#)). DAPI-stained ovaries were imaged individually, with an inverted Nikon microscope (x4 magnification), and each ovary was scored for the number of oocytes at stages 9–10 and 11–14.

Mitochondrial DNA quantification

DNA from ovaries (10 ovaries/sample) was extracted using UltraClean tissue and cell DNA isolation kit (MoBio), according to the manufacturer's instructions. Five ng of purified DNA was used for each PCR reaction. All reactions were performed in triplicates using SYBR green mix (Applied Biosystems) in 384-well plates on a ViiA7 Real-Time PCR system (Applied Biosystems).

Primer sequences for *mtDNA*, *RPL-32* and *Actin* are listed in [Table S1](#).

Quantitative RT-PCR

Total RNA from dissected tissues (ovaries, heads, gut, and mature oocytes) was extracted using Quick RNA microPep (Zymo). mRNA was converted to cDNA by a high-capacity reverse transcription kit (Thermo Fisher Scientific). Expression of representative mitochondrial genes was analyzed by qPCR reactions using fast SYBR green master mix (Applied Biosystems) in 384-well plates mounted on a

ViiA7 Real-Time PCR system (Applied Biosystems). Three replicates of 5ng cDNA/sample and 1.25ng cDNA/sample were used, respectively, for nuclear-encoded and mitochondria-encoded mitochondrial genes. Transcript levels were normalized to Actin5C DNA. Primer sequences for *Actin5C*, *Col*, *ND1*, *ATPase6*, *cytB*, *mtSSB*, *Milt*, *PMI*, *Tim8*, *ND-20*, *ND-SGDH* are listed in [Table S1](#).

ATP and ADP analysis by quantitative LC-MS/MS

Dissected tissues (ovaries, heads, and mature oocytes) were homogenized in 500μl of aqueous 70% methanol and agitated at 9°C in Thermo Mixer C (Eppendorf) for 10 min following addition of 5 μL of 1mM $^{13}\text{C}_{10}$ -ATP. Sample preparation and qLC-MS/MS (Waters Corp.) analysis were performed as described previously ([Lee et al., 2018](#)). Analytics were detected using multiple-reaction monitoring in positive ion mode and applying the parameters listed in [Table S2](#).

Measurements of mitochondrial membrane potential

Dissected ovaries of 6 day-old mito-EYFP females were incubated for 5 minutes with 10nM Tetramethyl rhodamine ethyl ester (TMRE; Sigma) in PBS and washed 4 times in PBS, as previously described in [Sieber et al. \(2016\)](#). Ovarioles were separated under a dissecting microscope and fluorescent images of TMRE (561nm) and EYFP (488nm) were acquired by confocal microscopy (Olympus FV1000). Egg chambers at early-mid stages (stages germarium-8) were imaged for each treatment. Quantitative analysis of TMRE and EYFP in follicle cells was performed by averaging pixel intensities in relevant regions using the Fiji/ImageJ software ([Schindelin et al., 2012](#)). Mitochondrial membrane potential was evaluated from the ratio between the average pixel intensities of TMRE and EYFP in the same region.

RNAi experiments

Flies carrying *UAS-siRNAs* were crossed with *Gal4-Tj* or *Gal4-NOS* lines. Offspring were transferred into new vials 1 day after eclosion. DAPI staining and ovary staging were performed on day 6, as described above.

Efficiency of RNAi inhibition test

For somatic cells, RNA was extracted, as described above, from ovaries containing 0-9 egg chamber stages of *tj>siCtrl*, *tj>siND-20*, *tj > siND-SGDH* females. For germline cells, RNA was extracted from mature oocytes of *NOS>siCtrl*, *NOS>siND-20*, *NOS > siND-SGDH* females following follicle cells removal as described in [Sieber et al. \(2016\)](#). Expression of *ND-20* and *ND-SGDH* was tested by quantitative RT-PCR, using specific primers, as described above.

Metabolomics and Lipidomics

Sample preparation

Lipid extraction was performed as previously described ([Malitsky et al., 2016](#)) with some modifications: ~50 females/pairs of ovaries were homogenized with 1ml of a pre-cooled methanol: methyl-tertbutyl-ether (TMBE) 1:3 (v/v) mixture containing internal standards (0.1 μg*ml⁻¹ of Phosphatidylcholine 34:0 (17:0/17:0) and 0.15nmol*ml⁻¹ of LM6002 (Avanti) standard mix). Following sonication for 30min in ice-cold sonication bath, with brief vortex every 10min, UPLC grade water: methanol (3:1, v/v) solution (0.5ml) was added and the samples were centrifuged. The upper organic phase was used for lipidomic analysis and the polar phase was re-extracted as described above, with 0.5ml of TMBE. Organic phases of the first and second extractions were combined and dried using speedvac.

Lipidomics analysis

Dried lipid extracts were re-suspended in 250 μL mobile phase B (see below) and centrifuged again at 13,000 rpm 4°C for 5min. The supernatant was transferred to an autosampler vial and subjected to UPLC-MS (Ultra performance liquid chromatography - mass spectrometry) analysis. Lipid extracts were analyzed using a Waters ACQUITY UPLC system coupled to a Vion IMS QToF mass spectrometer (Waters Corp.). Chromatographic conditions were as described by [Malitsky et al. \(2016\)](#) with small alterations. Briefly, the chromatographic separation was performed on an ACQUITY UPLC BEH C8 column (2.1 × 100mm, i.d., 1.7 μm) (Waters Corp.). The mobile phase A consisted of 45% water (UPLC grade) with 1% 1M NH₄Ac, 0.1% acetic acid and 55% acetonitrile: isopropanol (7:3) with 1% 1M NH₄Ac, 0.1% acetic acid (mobile phase B). The column was maintained at 40°C and flow rate of mobile phase was 0.4ml*min⁻¹. Mobile phase A was run for 1 min at 100% and then gradually reduced to 25% over 12min, followed by 4min of decrease to 0%. Mobile phase B was run at 100% till the 21min, and mobile phase A was set to 100% at minute 21.5. Finally, column was equilibrated at 100% A until the 25th minute. MS parameters were as follows: Source and de-solvation temperatures were maintained at 120°C and 450°C, respectively; capillary voltages were set to 3.0 kV and 2 kV for positive and negative ionization mode, respectively; cone voltage was set to 40 V. Nitrogen was used as de-solvation gas and cone gas at the flow rate of 800L*h⁻¹ and 30L*h⁻¹, respectively. The mass spectrometer was operated in full scan HDMS^E positive resolution mode over a mass range of 50–1800Da. For high energy scan function, collision energy ramp of 20–60eV was applied, and low energy scan function was performed with 4eV was applied. Leucine-enkephalin was used as lock-mass reference standard.

Analysis of polar metabolites

Metabolic profiling of polar phase was done as previously described ([Zheng et al., 2015](#)) with minor modifications. Briefly, analysis was performed using Aquity I class UPLC System combined with mass spectrometer (Thermo Exactive Plus Orbitrap), operated in a

negative ionization mode. LC separation was done using SeQuant Zic-pHilic (150mm × 2.1mm) with the SeQuant guard column (20mm × 2.1mm) (Merck). The Mobile phase A: acetonitrile and Mobile phase B: 20mM ammonium carbonate plus 0.1% ammonia hydroxide in water. Flow rate was kept at 200 $\mu\text{l min}^{-1}$ and the gradient was as follow: 0-2min 75% of B, 17min 12.5% of B, 17.1min 25% of B, 19min 25% of B, 19.1min 75% of B, 19min 75% of B.

Metabolite identification

Lipid LC-MS data were analyzed and processed with UNIFI (Version 1.9.2, Waters Corp., MA, USA). Putative identification of lipid species was performed by comparison accurate mass, fragmentation pattern, and ion mobility (CCS) values to in-house made lipid database, as well as to standards, when available. Further annotation of lipids was based on correlation between retention time (RT) and carbon chain length and degree of unsaturation. Validation of lipid identification was performed by matchup with home-made library, composed of defined lipids from various organisms. Processing of polar metabolite data was done using TraceFinder Thermo Fisher software. Detected compounds were identified by retention time and fragments were further verified using in-house mass spectra library.

QUANTIFICATION AND STATISTICAL ANALYSIS

Statistical analyses were performed using “Prism 5” (Graphpad Software). Statistical analysis of normally distributed data was analyzed by unpaired t test or ANOVA with Tukey’s multiple comparison test. Analysis of non-normal distributions was performed using Mann Whitney test or non-parametric ANOVA (Kruskal-Wallis) with Dunn’s multiple comparison test. Other details on statistical analysis can be found in Figure legends.

Metabolic statistical analysis

Peak intensities of polar and lipid metabolites were normalized twice: first to the relevant internal standards and then either to the number of flies (or ovaries) in each biological sample or to the sample’s weight (mg). The MetaboAnalyst 4.0 ([Chong et al., 2018](#)) was used for statistical analysis of differences in metabolites between groups, identification of altered metabolic pathways and heat-map visualizations

Permutation analysis

Unbiased statistical analysis of significant enrichment of specific metabolic pathways was performed by evaluating making 10000 selections of the same number of metabolites chosen at random and measuring the frequency at which the average log fold-change of the random set exceeds the average of the correct choice of metabolites within the respective pathway. This analysis was applied to log fold-changes in whole body and ovary of germ-free versus untreated females (GF versus Ctrl) and same for bacterial re-colonization versus germ-free (GF +bac versus GF).

Cell Reports, Volume 34

Supplemental Information

**Systemic Regulation of Host Energy and Oogenesis
by Microbiome-Derived Mitochondrial Coenzymes**

Yulia Gnainsky, Nofar Zfanya, Michael Elgart, Eman Omri, Alexander Brandis, Tevie Mehlman, Maxim Itkin, Sergey Malitsky, Jerzy Adamski, and Yoav Soen

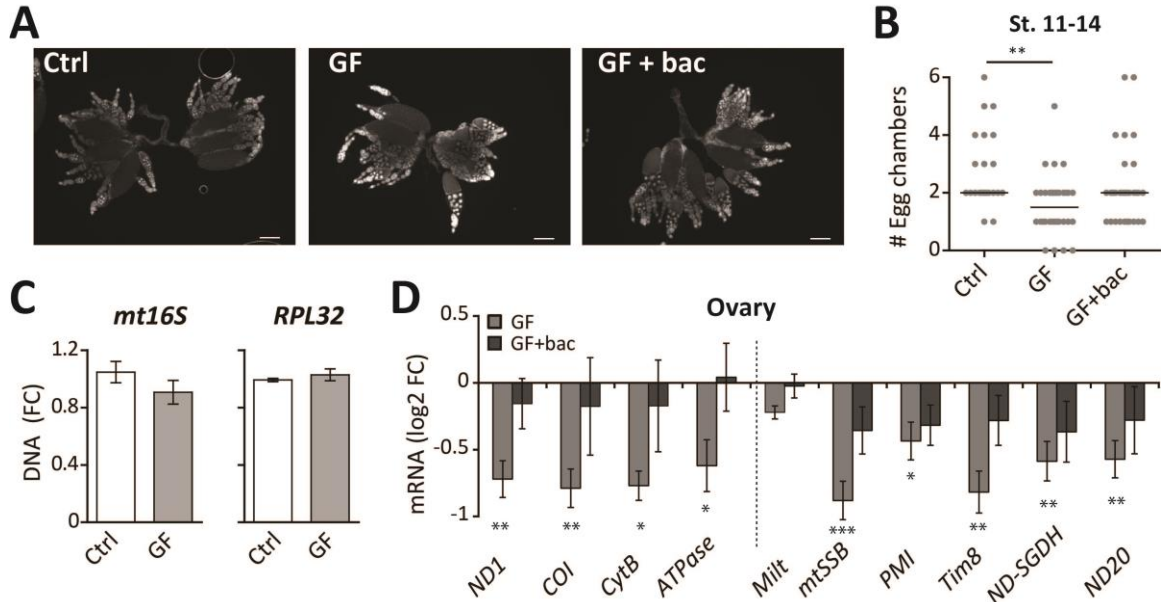


Figure S1. Reduced mitochondrial DNA and RNA in ovaries of young GF females vs. control, Related to Figure 1

(A) Representative images of DAPI-stained ovaries in 2 day-old yw females, shown for the following cases: conventionally raised (Ctrl) and germ free females with and without supplementation of native gut bacteria to the female diet (GF+bac and GF, respectively). Scale bar 200 μ m.

(B) Number of egg chambers at stages 11-14 in ovary for the cases shown in (A). Scatter dot plot and median; $n > 22$ ovaries; $**p < 0.01$ (Kruskal wallis with Dunn's multiple comparison test).

(C) Relative DNA levels (Fold-change, FC) of mitochondrial 16S (*mt16S*) and ribosomal protein L32 (*RPL32*) in ovaries of GF vs. control females, as determined by qPCR with *Drosophila* actin DNA as a reference. Mean \pm SEM, $n = 6$ with 10 ovaries per sample.

(D) mRNA fold change (log2 FC) of mitochondria-encoded (*ND1*, *COI*, *CytB*, *ATPase*) and nucleus-encoded mitochondrial genes (*Milt*, *mtSSB*, *Tim8*, *PMI*, *ND-SGDH*, *ND-20*) in ovaries of 2-day GF females vs. Ctrl. Mean \pm SE, $n > 6$ with 10 ovaries per sample; $*p < 0.05$, $**p < 0.01$, $***p < 0.001$ vs. Ctrl (t-test). *ND1*, NADH-ubiquinone oxidoreductase chain 1; *COI*, cytochrome C oxidase; *cytB*, cytochrome B; *Milt*, Milton; *mtSSB*, mitochondrial single stranded DNA-binding protein; *PMI*, protein of the mitochondrial inner membrane; *ND-SGDH*, NADH dehydrogenase (ubiquinone) SGD subunit; *ND-20*, NADH dehydrogenase (ubiquinone) 20kDa subunit.

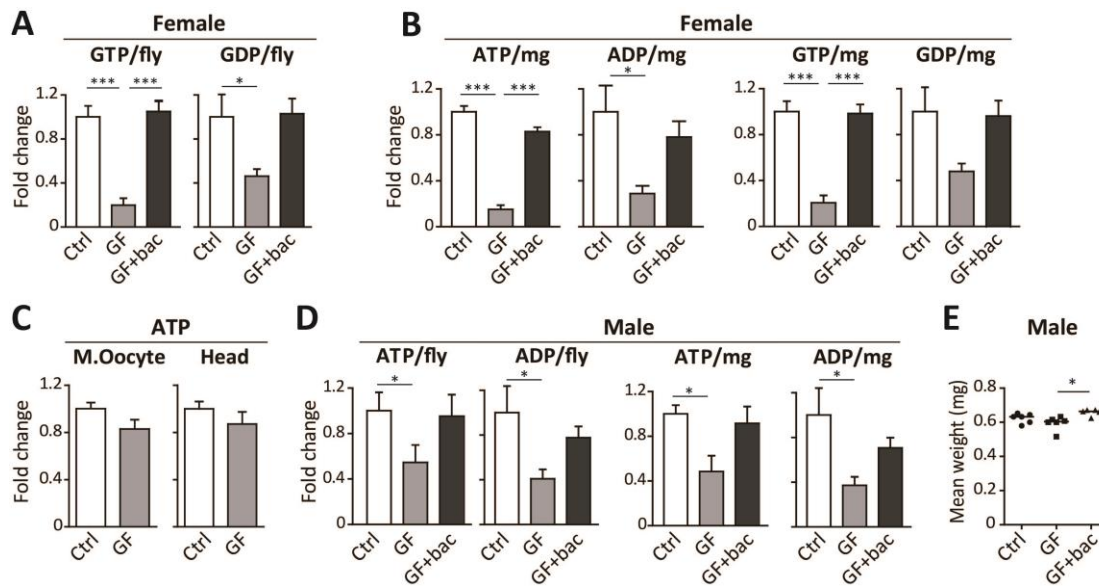


Figure S2. Reduced levels of GTP, GDP, ATP and ADP levels in GF females and males, Related to Figure 1

(A) Relative levels of GTP and GDP, measured by quantitative LC-MS in whole body of conventionally raised females (Ctrl) and GF females (day-6) with and without supplementation of native gut bacteria (GF + bac and GF, respectively). Mean \pm SEM, $n=5$, with ~ 50 flies/sample; * $p<0.05$, *** $p<0.001$ (ANOVA, followed by Tukey's test).

(B) Same as (A) for ATP, ADP, GTP and GDP levels, normalized by sample weight. Mean \pm SEM, $n=5$ with ~ 50 flies/sample; * $p<0.05$, *** $p<0.001$ (ANOVA with Tukey's multiple comparison test).

(C) ATP levels in mature oocytes (M.Oocyte) and heads of conventionally raised (Ctrl) and GF females. Mean \pm SEM, $n=8$ for mature oocytes (30 oocytes/sample) and $n=9$ for heads (10 heads/sample).

(D) Same as (B) for 6-day old males. Mean \pm SEM, $n=5-6$, with ~ 50 flies/sample; * $p<0.05$ (ANOVA with Tukey's test).

(E) Average male weight (mg) for the cases in (D); * $p<0.05$ (Kruskal Wallis with Dunn's multiple comparison test).

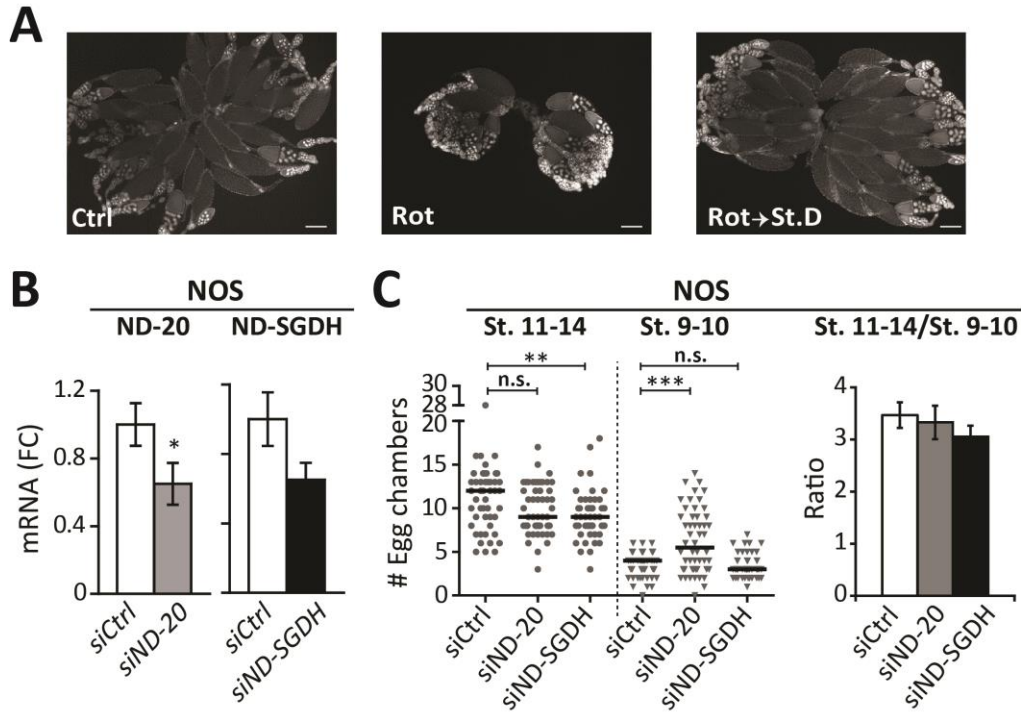


Figure S3. Effect of global and germ-line specific inhibition of mitochondrial function on the ovaries, Related to Figure 2

(A) Representative images of day-6 DAPI-stained ovaries of conventionally raised females (yw) for the following cases: no treatment (Ctrl), rotenone exposure (25 μ M) from day 3 to 6, with and without subsequent transfer to rotenone-free diet for 3 additional days (Rot and Rot \rightarrow Std. Diet, respectively). Scale bar 200 μ m.

(B) mRNA fold change of ND-20 and ND-SGDH, in dechorionated mature oocytes of *NOS>siCtrl*, *NOS>siND-20* and *NOS>siND-SGDH* females. Mean \pm SEM, $n \geq 4$ (~30 oocytes per sample);

* $p < 0.05$ (t-test).

(C) Left: Number of egg chambers at stages 11-14 and 9-10 in ovaries of *NOS>siCtrl*, *NOS>siND-20* and *NOS>siND-SGDH* females. Right: Ratio between the numbers of chambers in 11-14th vs. 9-10th stage. Mean \pm SEM; $n = 46-52$ ovaries; ** $p < 0.01$, *** $p < 0.001$ versus *NOS>siCtrl* (Mann Whitney test).

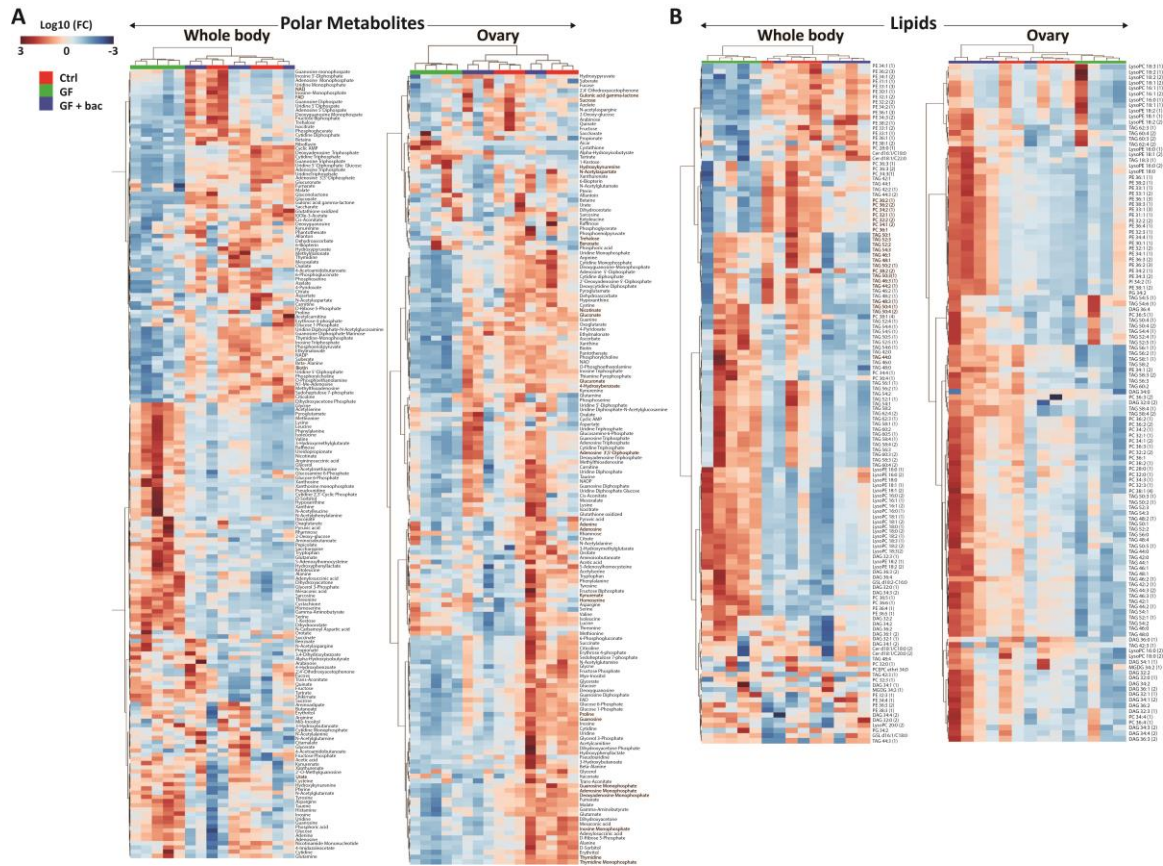


Figure S4. Hierarchical clustering of polar and lipid metabolites, Related to Figure 4
(A, B) Relative abundance of polar metabolites (A) and lipids (B) measured by LC-MS in whole body and ovary of 6-day conventionally raised (Ctrl) and germ-free (GF), with and without supplementation of native gut bacteria (GF+bac and GF, respectively). Color code corresponds to log₁₀ fold-change versus Ctrl, with each row and column corresponding, respectively, to a specific metabolite and a particular sample.

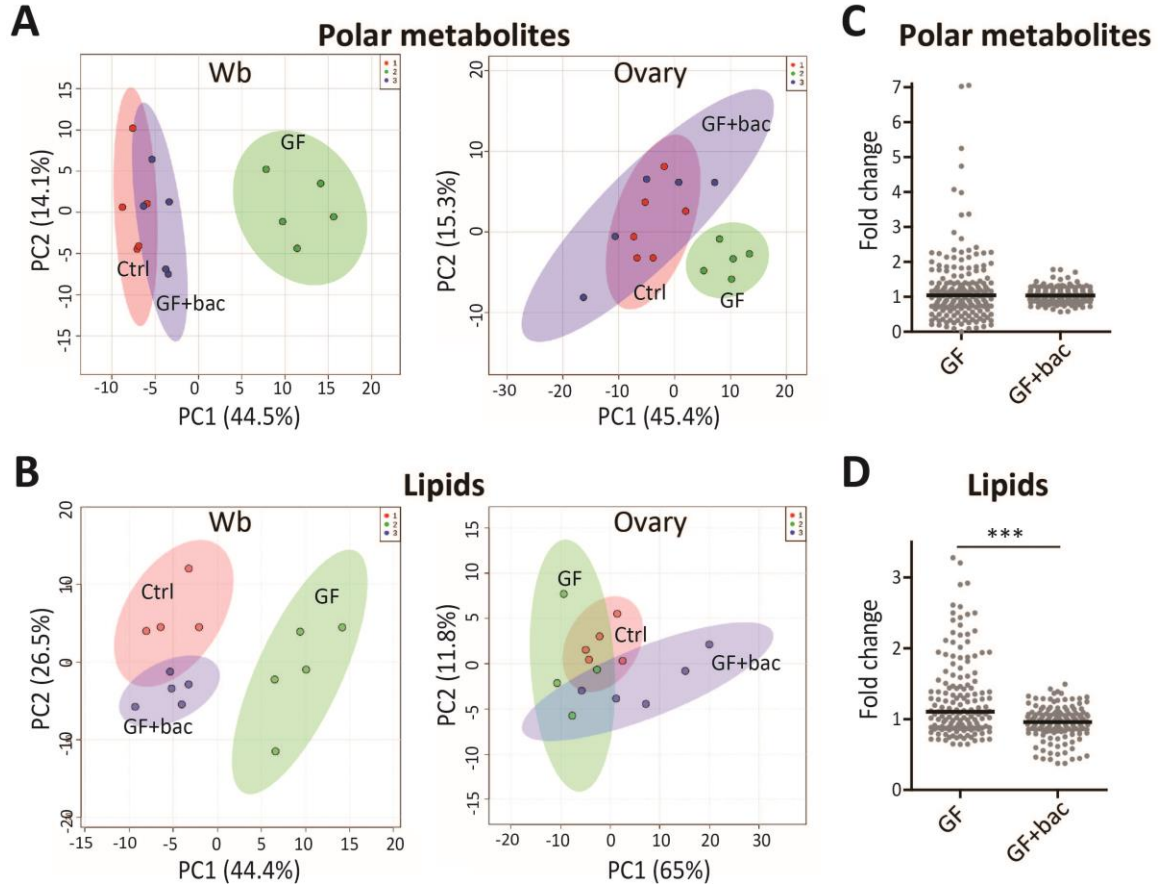


Figure S5. Global analysis of metabolic changes, Related to Figure 4

(A, B) Principle component analysis (PCA) of polar metabolites (A) and lipids (B), based on LC-MS measurements in whole body (Wb) and ovary samples of day-6 conventionally raised (Ctrl) and germ free females, with and without supplementation of native gut bacteria (GF+bac and GF, respectively). n=5-6; ~50 females/ovaries per sample.

(C, D) Fold change (versus control) shown for all the polar (C) and lipid metabolites (D) in whole-body of GF females, with and without bacterial supplementation (GF+bac and GF, respectively). Each dot corresponds to the average fold-change of a specific metabolite; Scatter dot plot with medians; *** $p < 0.001$ (Mann Whitney test).

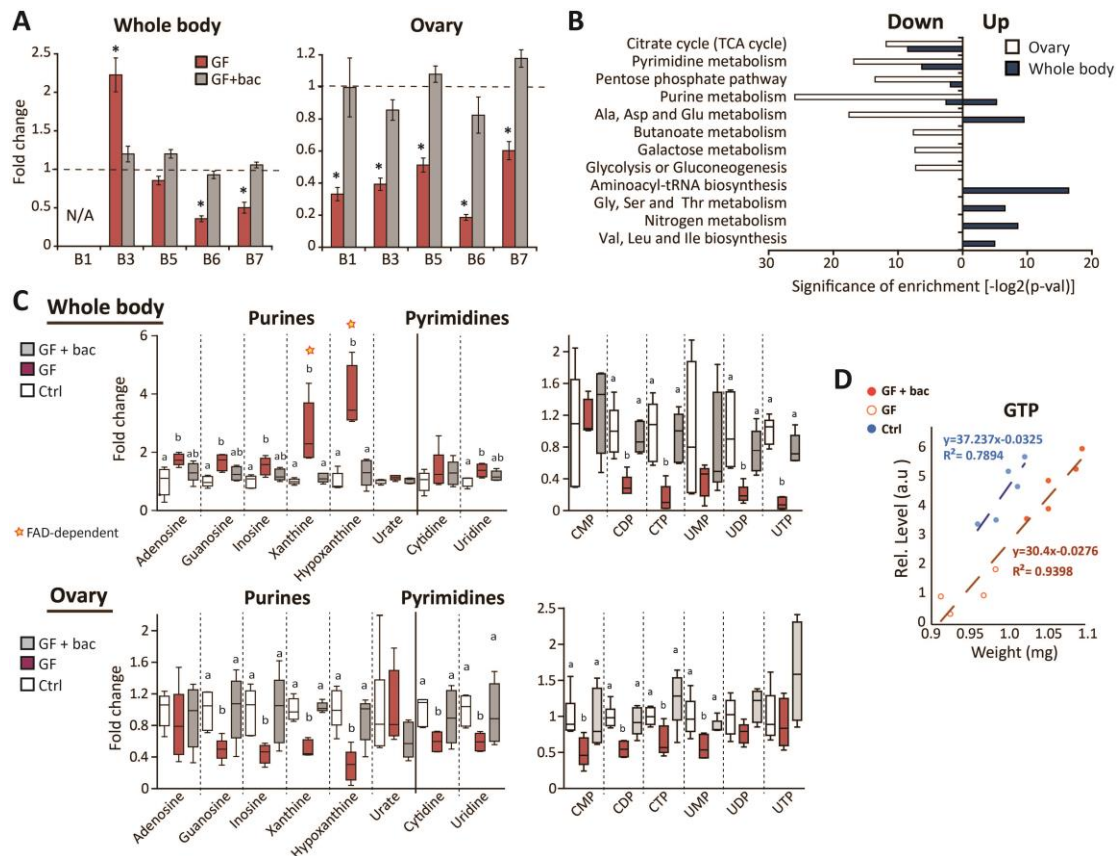


Figure S6. Impact of gut bacteria on B-type vitamins, purines and pyrimidines, Related to Figure 4

(A) Fold change of B-type vitamins in whole body and ovary of day 6 GF females with and without bacterial supplementation (GF+bac and GF), relative to conventionally raised females (Ctrl, dashed line). Mean \pm SEM; $n=5-6$; ~ 50 females/ovaries per sample. *FDR<0.05 (ANOVA with Tukey's multiple comparison test).

(B) Pathway enrichments in sets of polar metabolites that increase (Up) and decrease (Down) in whole body and ovary of GF vs. conventionally raised females. Significance of enrichment is displayed as -log2 of FDR determined by hypergeometric test.

(C) Fold change of purines and pyrimidines in whole body (upper panels) and ovary (lower panels) for the cases in (A). Median \pm quartiles; medians sharing a letter are not significantly different (ANOVA with Tukey's multiple comparison test, FDR<0.05).

(D) Scatter plot of GTP (arbitrary units, a.u. of peak intensity) against weight of females for the cases in (A).

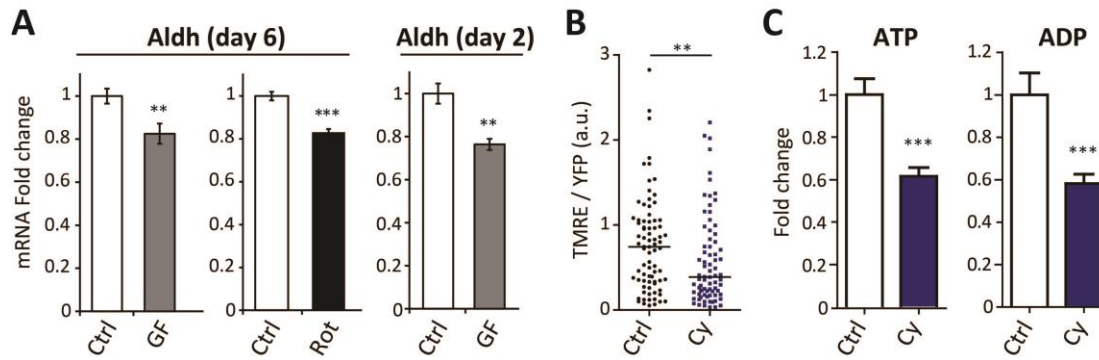


Figure S7. Crosstalk between *Aldh* and mitochondrial functions, Related to Figure 1

(A) Left panel: Changes in *Aldh* mRNA levels in ovaries of conventionally raised females (Ctrl), rotenone-treated females (Rot, 25 μ M) and GF females. Right panel: *Aldh* fold-change in young (day-2) conventionally raised (Ctrl) and germ free (GF) females. Mean \pm SE; n>6; ** p<0.01, *** p<0.001 (t-test).

(B) TMRE/EYFP intensity ratio (arbitrary units, a.u.) in follicle cells of 6-8 stage egg chambers of conventionally raised and cyanamide-treated females. Scatter dot plot with medians; n>77; 3 independent experiments. **p<0.01 (Man Whitney test).

(C) ATP and ADP fold-change, measured by quantitative LC-MS in ovaries of day 6 conventionally raised (Ctrl) and 3mM cyanamide-treated females (CY). Mean \pm SE; 4 independent experiments; n \geq 13; *** p<0.001 (t-test).

Table S1. Primers used in this study, Related to Star Methods

Target gene	Forward primer	Reverse primer	Related to Figures
<i>mtDNA 16S</i>	AAAAAGATTGCGACCTCGAT	AAACCAACCTGGCTTACACC	1D and S1C
<i>RPL-32</i>	AGGCCCAAGATCGTGAAGAA	TGTGCACCAGGAACTTCTTGAA	S1C
<i>Actin</i>	GGAAACCACGCAAATTCTCAGT	CGACAACCAGAGCAGCAACTT	1D and S1C
<i>Actin5C</i>	CCCTCGTTCTTGGGAATGG	CGGTGTTGGCATAACAGATCCT	1F,1G and S1D
<i>Col</i>	TGAACAGTACCTGCTTTAGGAGT	TGACCATAAAATAAACCCGGTCG	1F,1G and S1D
<i>ND1</i>	CCTCAACCTTTTTGTGATGCG	GACGACCAACCAGCTACTATAAC	1F,1G and S1D
<i>ATPase6</i>	TTTTCTGTATTGACCCCTTAGC	GATCCATTATGACCTGATGGTCC	1F,1G and S1D
<i>cytB</i>	ACTCCTTTAGTAACACCTGCCC	TGGTCGAGCTCCAATTCAAGT	1F,1G and S1D
<i>mtSSB</i>	GTCACCTTTTCGGTTGCTACA	GCTTGAACACCACTACACGATG	1F,1G and S1D
<i>Milt</i>	GCAGACGATGGCACAGATACT	CGTCGAGCAGGGAGTTGAC	1F,1G and S1D
<i>PMI</i>	CTGGACAAGGCGCTGGAA	CAAATCCAACGACCAGTTTCG	1F,1G and S1D
<i>Tim8</i>	AACCTTTCCGGCAATGACAAG	CCGATGCACTTCTCCCAGC	1F,1G and S1D
<i>ND-20^a</i>	CGTGGCTGCGATAGGATAAT	ACCACATCTGGAGCGTCTTC	1F,1G, 2I, S1D, S3B
<i>ND-SGDH^a</i>	AGTCACCGCATTGGTTCTCT	GAGATGGGGTGCTTCTCGTA	1F,1G, 2I, S1D, S3B

^aPrimer sequences from Copeland et al. (Copeland et al., 2009)

Table S2. Parameters for quantitative LC-MS/MS based analysis of ATP and ADP levels, Related to Star methods

Name of the compound	Retention time, min	Transition, m/z	Cone voltage, V	Collision energy, eV	LOQ (10ng/ml)
ADP	1.33	428.0 > 136.1	25	25	10
		428.0 > 348.1	25	14	
ATP	1.54	507.9 > 136.0	14	35	10
		507.9 > 410.0	14	18	